



Institutional Sign In

All



Search within Publication

ADVANCED SEARCH

Author Resources

Submission Guidelines

Browse Journals & Magazines -> IEEE Transactions on Biomedica...

Submit Manuscript

IEEE Transactions on Biomedical Circuits and Systems

Author Center



Submit Manuscript



Add Title To My Alerts



Add to My Favorites



Become a Reviewer

Home Popular Open Access Publishing Options

Early Access

Current Issue

All Issues

About Journal

Meet the Editor **0.00675**
Editor-in-Chief Eigenfactor

1.119
Article Influence Score

9.6
CiteScore
Powered by Scopus

Kea-Tiong (Samuel) Tang
National Tsing Hua University
E-mail: kttang@ee.nthu.edu.tw

Aims & Scope

The *IEEE Transactions on Biomedical Circuits and Systems* (TBioCAS) addresses areas at the crossroads of Circuits and Systems and Life Sciences. The main emphasis is on microelectronic issues in a wide range of applications found in life sciences, physical sciences and engineering. The primary goal of the journal is to bridge the unique scientific and technical activities of the IEEE Circuits and Systems Society to a wide variety of related areas.

General, theoretical, and application-oriented papers in the biomedical technical area with a Circuits and Systems perspective are encouraged for publication in TBioCAS. To be considered in scope, submissions to TBioCAS must demonstrate synergies between circuits and systems and medicine/biology.

The articles in this journal are peer reviewed in accordance with the requirements set forth in the IEEE PSPB Operations Manual (sections 8.2.1.C & 8.2.2.A). Each published article was reviewed by a minimum of two independent reviewers using a single-blind peer review process, where the identities of the reviewers are not known to the authors, but the reviewers know the identities of the authors. Articles will be screened for plagiarism before acceptance.

Corresponding authors from low-income countries are eligible for waived or reduced open access APCs.

Indexed in Pubmed® and Medline®, products of the United States National Laboratory of Medicine



Author Resources

Submission Guidelines

Submit Manuscript

Author Center

Become a Reviewer

Open Access Publishing Options

Meet the Editor

Editor-in-Chief

Kea-Tiong (Samuel) Tang
National Tsing Hua University
E-mail: kttang@ee.nthu.edu.tw

Publication Details

Subjects



IEEE TRANSACTIONS ON BIOMEDICAL CIRCUITS AND SYSTEMS

The IEEE TRANSACTIONS ON BIOMEDICAL CIRCUITS AND SYSTEMS is published by the IEEE Circuits and Systems Society and the IEEE Engineering in Medicine and Biology Society. For membership and subscription information and pricing, please visit www.ieee.org/membership-catalog.

SPONSORING SOCIETIES

Circuits and Systems

AMARA AMARA, *President*

Editor-in-Chief

KEA-TIONG (SAMUEL) TANG
National Tsing Hua University
Hsinchu, Taiwan

Engineering in Medicine and Biology

SHANKAR SUBRAMANIAM, *President*

Associate Editor-in-Chief

PEDRAM MOHSENI
Case Western Reserve University
Cleveland, OH, USA

Associate Editor-in-Chief

ROBERT RIEGER
University of Kiel
Kiel, Germany

Associate Editors

ARINDAM BASU
City University of Hong Kong
Hong Kong, China

MAIDE BUCCOLO
University of Catania
Catania, CT, Italy

ALISON BURDETT
Sensium-Healthcare
Abingdon, Oxford, UK

MARCO CARMINATI
Politecnico di Milano
Milano, Italy

SANDRO CARRARA
École polytechnique fédérale
de Lausanne
Lausanne, Switzerland

JIE CHEN
University of Alberta
Edmonton, AB, Canada

VANESSA CHEN
Carnegie Mellon University
Pittsburgh, PA, USA

SHIH-WEN CHIU
Enosim Biotech
Hsinchu, Taiwan

TIAGO COSTA
Delft University of Technology
Delft, Netherland

JOHN DEEPU
University College Dublin
Dublin, Ireland

ANDREAS DEMOSTHENOUS
University College London
London, UK

PANTELIS GEORGIU
Imperial College London
London, UK

SARA GHOREISHIZADEH
University College London
London, UK

MAYSAM GHOVANLOO
Bionic Sciences Inc
Atlanta, GA, USA

BENOIT GOSSELIN
University Laval
Quebec, QC, Canada

ULKUHAN GULER
Worcester Polytechnic Institute
Worcester, MA, USA

SOHMYUNG HA
New York University
Abu Dhabi

DREW HALL
University of California San Diego
San Diego, USA

HADI HEIDARI
University of Glasgow
Scotland, UK

ANNE HEURTIER
University of Angers
Angers, France

YUANQI HU
Beihang University
Beijing, China

CHUNG-CHIH HUNG
National Yang Ming Chiao Tung
University
Hsinchu, Taiwan

YAOLIAO JIA
The University of Texas at Austin
Austin, TX, USA

HANJUN JIANG
Tsinghua University
Beijing, China

MATTHEW JOHNSTON
Oregon State University
Corvallis, OR, USA

MEHDI KIANI
Penn State University
University Park, PA, USA

CHUL KIM
KAIST
Daejeon, Korea

SANG JOON KIM
Samsung Electronics
Suwon, Korea

EDMUND LAM
University of Hong Kong
Hong Kong, China

SHUENN-YUH LEE
National Cheng Kung
University
Tainan, Taiwan

LI WEN
Michigan State University
East Lansing, MI, USA

YONGFU LI
Shanghai Jiao Tong University
Shanghai, China

NICOLE MCFARLANE
University of Tennessee
Knoxville, TN, USA

WOUTER SERDIJN
Delft University of Technology
Delft, Netherland

SAMEER SONKUSALE
Tufts University
Medford, MA, USA

WEI TANG
New Mexico State University
Las Cruces, NM, USA

TAKASHI TOKUDA
Tokyo Institute of Technology
Tokyo, Japan

JERALD YOO
National University of Singapore
Singapore, Singapore

YUANJIN ZHENG
Nanyang Technological University
Singapore, Singapore

K. J. RAY LIU, *President & CEO*

SAIFUR RAHMAN, *President-Elect*

KATHLEEN A. KRAMER, *Director & Secretary*

JOHN W. WALZ, *Director & Treasurer*

SUSAN "KATHY" LAND, *Past President*

IEEE Officers

STEPHEN M. PHILLIPS, *Director & Vice President, Educational Activities*

LAWRENCE O. HALL, *Director & Vice President, Publication Services and Products*

DAVID A. KOEHLER, *Director & Vice President, Member and Geographic Activities*

JAMES E. MATTHEWS, *Director & President, Standards Association*

BRUNO MEYER, *Director & Vice President, Technical Activities*

DEBORAH M. COOPER, *Director & President, IEEE-USA*

FRANCO MALOBERTI, *Director & Delegate, Division I*

IEEE Executive Staff

STEPHEN WELBY, *Executive Director & Chief Operating Officer*

THOMAS SIEGERT, *Finance and Administration*

DONNA HOURICAN, *Staff Executive, Corporate Activities*

JAMIE MOESCH, *Managing Director, Educational Activities*

SOPHIA A. MUIRHEAD, *General Counsel & Chief Compliance Officer*

CHRIS BRANTLEY, *Managing Director, IEEE-USA*

CHERIF AMIRAT, *Chief Information Officer*

KAREN HAWKINS, *Chief Marketing Officer*

CECELIA JANKOWSKI, *Managing Director, Member and Geographic Activities*

STEVEN HEFFNER, *Publications*

KONSTANTINOS KARACHALIOS, *Managing Director, IEEE-Standards Association*

MARY WARD-CALLAN, *Managing Director, Technical Activities*

IEEE Publishing Operations

Senior Director, Publishing Operations: DAWN MELLELY

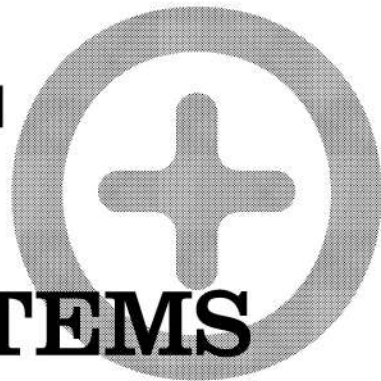
Director, Editorial Services: KEVIN LISANKIE *Director, Production Services:* PETER M. TUOHY

Associate Director, Editorial Services: JEFFREY E. CICHOCKI *Associate Director, Information Conversion and Editorial Support:* NEELAM KHINVASARA

Senior Manager, Journals Production: KATIE SULLIVAN *Journals Production Manager:* SARA T. SCUDDER

IEEE TRANSACTIONS ON BIOMEDICAL CIRCUITS AND SYSTEMS (ISSN 1932-4545) is published bimonthly by The Institute of Electrical and Electronics Engineers, Inc. Responsibility for the contents rests upon the authors and not upon the IEEE, the Society/Council, or its members. **IEEE Corporate Office:** 3 Park Avenue, 17th Floor, New York, NY 10016. **IEEE Operations Center:** 445 Hoes Lane, Piscataway, NJ 08854. **NJ Telephone:** +1 732 981 0060. **To order individual copies for members and nonmembers, please email the IEEE Contact Center at contactcenter@ieee.org.** Member and nonmember subscription prices available upon request. **Copyright and Reprint Permissions:** Abstracting is permitted with credit to the source. Libraries are permitted to photocopy for private use of patrons, provided the per-copy fee of \$31.00 is paid through the Copyright Clearance Center, 222 Rosewood Drive, Danvers, MA 01923. For all other copying, reprint, or republication permission, write to Copyrights and Permissions Department, IEEE Publications Administration, 445 Hoes Lane, Piscataway, NJ 08854. Copyright © 2020 by The Institute of Electrical and Electronics Engineers, Inc. All rights reserved. Periodicals Postage Paid at New York, NY and at additional mailing offices. **Postmaster:** Send address changes to IEEE TRANSACTIONS ON BIOMEDICAL CIRCUITS AND SYSTEMS, IEEE, 445 Hoes Lane, Piscataway, NJ 08854. GST Registration No. 125634188. CPC Sales Agreement#40013087. Return undeliverable Canada addresses to: Pitney Bowes IMEX, P.O. Box 4332, Stanton Rd., Toronto, ON M5W 3J4, Canada. IEEE prohibits discrimination, harassment and bullying. For more information visit <http://www.ieee.org/nondiscrimination>. Printed in U.S.A.

IEEE TRANSACTIONS ON BIOMEDICAL CIRCUITS AND SYSTEMS



A PUBLICATION OF THE IEEE CIRCUITS AND SYSTEMS SOCIETY  
IEEE ENGINEERING IN MEDICINE AND BIOLOGY SOCIETY

Indexed in PubMed® and MEDLINE®, products of the United States National Library of Medicine



OCTOBER 2022 VOLUME 16 NUMBER 5 ITBCCW (ISSN 1932-4545)

SPECIAL SECTION ON THE 2022 INTERNATIONAL SYMPOSIUM ON INTEGRATED CIRCUITS AND SYSTEMS (ISICAS)

GUEST EDITORIAL
 Editorial.....*H. Heidari, Y. Jia, and B. Zhao* 730

SPECIAL SECTION PAPERS

An Energy-Efficient Bridge-to-Digital Converter for Implantable Pressure Monitoring Systems.....
*M. Besirli, K. Ture, M. Beghetti, C. Dehollain, M. Mattavelli, F. Maloberti, and D. Barrettino* 732

A 0.8- μ W and 74-dB High-Pass Sigma-Delta Modulator With OPAMP Sharing and Noise-Coupling Techniques for Biomedical Signal Acquisition.....*S.-Y. Lee, H.-Y. Lee, C.-H. Kung, P.-H. Su, and J.-Y. Chen* 742

A Fully Implantable Opto-Electro Closed-Loop Neural Interface for Motor Neuron Disease Studies.....
*F. Liu, Y. Wu, N. Almarri, M. Habibollahi, H. T. Lancashire, B. Bryson, L. Greensmith, D. Jiang, and A. Demosthenous* 752

A 10 M Ω , 50 kHz-40 MHz Impedance Measurement Architecture for Source-Differential Flow Cytometry.....
*B. Shen, J. Dawes, and M. L. Johnston* 766

Spintronic Eyeblink Gesture Sensor With Wearable Interface System.....
*A. Tanwear, X. Liang, E. Paz, T. Böhnert, R. Ghannam, R. Ferreira, and H. Heidari* 779

A 2.66 μ W Clinician-Like Cardiac Arrhythmia Watchdog Based on P-QRS-T for Wearable Applications.....
*X. Xu, Q. Cai, Y. Zhao, G. Wang, L. Zhao, and Y. Lian* 793

A High-Accuracy and Energy-Efficient CORDIC Based Izhikevich Neuron With Error Suppression and Compensation.....
*J. Wang, Z. Peng, Y. Zhan, Y. Li, G. Yu, K.-S. Chong, and C. Wang* 807

Low Complexity Binarized 2D-CNN Classifier for Wearable Edge AI Devices.....
*D. L. T. Wong, Y. Li, D. John, W. K. Ho, and C.-H. Heng* 822

An Ultra-Energy-Efficient and High Accuracy ECG Classification Processor With SNN Inference Assisted by On-Chip ANN Learning.....
*R. Mao, S. Li, Z. Zhang, Z. Xia, J. Xiao, Z. Zhu, J. Liu, W. Shan, L. Chang, and J. Zhou* 832

(Contents Continued on Page 729)



An Ultrasonic Energy Harvesting IC Providing Adjustable Bias Voltage for Pre-Charged CMUT	842
..... <i>L. Zhao, M. Annayev, Ö. Oralkan, and Y. Jia</i>	
An Intra-Body Power Transfer System With >1-mW Power Delivered to the Load and 3.3-V DC Output at 160-cm of on-Body Distance	852
..... <i>H. Cho, J.-H. Suh, C. Kim, S. Ha, and M. Je</i>	

REGULAR PAPERS

SPRSound: Open-Source SJTU Paediatric Respiratory Sound Database	
..... <i>Q. Zhang, J. Zhang, J. Yuan, H. Huang, Y. Zhang, B. Zhang, G. Lv, S. Lin, N. Wang, X. Liu, M. Tang, Y. Wang, H. Ma, L. Liu, S. Yuan, H. Zhou, J. Zhao, Y. Li, Y. Yin, L. Zhao, G. Wang, and Y. Lian</i>	867
Frequency Error Compensation of Unsynchronized Bistatic CW- MIMO Radar for Multiple Human-Body Localization	882
..... <i>A. Abuduaini, N. Shiraki, N. Honma, T. Nakayama, and S. Iizuka</i>	
Derivation of Bioimpedance Model Data Utilizing a Compact Analyzer and Two Capacitive Electrodes: A Forearm Example	891
..... <i>J. Ojarand, E. Priidel, and M. Min</i>	
EMCI: A Novel EEG-Based Mental Workload Assessment Index of Mild Cognitive Impairment	902
..... <i>H. Zeng, X. Fang, Y. Zhao, J. Wu, M. Li, H. Zheng, F. Xu, D. Pan, and G. Dai</i>	
A Wearable Capsule Endoscope Electromagnetic Localization System Based on a Novel WCL Algorithm	915
..... <i>C. Xiao, Z. Liang, and X. Jiang</i>	
Memristive Circuit Implementation of Operant Cascaded With Classical Conditioning	926
..... <i>C. Yang, X. Wang, Z. Chen, S. Zhang, and Z. Zeng</i>	
Efficient Power Receiving Coil With Novel Ferrite Core Structure for Capsule Robot	939
..... <i>H. Zhuang, W. Wang, K. Zhao, S. Kuang, Z. Wang, and G. Yan</i>	
Respinos: A Portable Device for Remote Vital Signs Monitoring of COVID-19 Patients	
..... <i>T. Adiono, N. Ahmadi, C. Saraswati, Y. Aditya, Y. P. Yudhanto, A. Aziz, L. Wulandari, D. Maranatha, G. Khusnurrokhman, A. R. W. Riadi, and R. W. Sudjud</i>	947
Bioimpedance Measurement of Knee Injuries Using Bipolar Electrode Configuration	962
..... <i>X. Ye, L. Wu, K. Mao, Y. Feng, J. Li, L. Ning, and J. Chen</i>	
Integrated Hybrid Sub-Aperture Beamforming and Time-Division Multiplexing for Massive Readout in Ultrasound Imaging	972
..... <i>A. Rezvanitabar, G. Jung, C. Tekes, T. M. Carpenter, D. M. J. Cowell, S. Freear, and F. L. Degertekin</i>	
Extraction of Fetal ECG From Abdominal and Thorax ECG Using a Non-Causal Adaptive Filter Architecture	981
..... <i>Edwin Dhas D and Suchetha M</i>	

Respinos: A Portable Device for Remote Vital Signs Monitoring of COVID-19 Patients

Trio Adiono[✉], *Member, IEEE*, Nur Ahmadi[✉], *Member, IEEE*, Citrya Saraswati, Yudi Aditya, Yusuf Purna Yudanto, Abdillah Aziz, Laksmi Wulandari, Daniel Maranatha, Gemilang Khusnurrokhman, Agustinus Rizki Wirawan Riadi, and Reza Widiyanto Sudjud

Abstract—The rapidly increasing number of COVID-19 patients has posed a massive burden on many healthcare systems worldwide. Moreover, the limited availability of diagnostic and treatment equipment makes it difficult to treat patients in the hospital. To reduce the burden and maintain the quality of care, asymptomatic patients or patients with mild symptoms are advised to self-isolate at home. However, self-isolated patients need to be continuously monitored as their health can turn into severe/critical condition within a short period of time. Therefore, a portable device that can remotely monitor the condition and progression of the health of these patients is urgently needed. Here we present a portable device, called Respinos, that can monitor multiparameter vital signs including respiratory rate, heart rate, body temperature, and SpO₂. It can also operate as a spirometer that measures forced vital capacity (FVC), forced expiratory volume (FEV), FEV in the first second (FEV₁), and peak expiratory flow Rate (PEFR) parameters which are useful for detecting pulmonary diseases. The spirometer is designed in the form of a tube that can be ergonomically inflated by the patient, and is equipped with an accurate and disposable turbine based air flow sensor to evaluate the patient's respiratory condition. Respinos uses rechargeable batteries and wirelessly connects to a mobile application whereby the patient's condition can be monitored in real-time and consulted with doctors via chat. Extensive comparison against medical-grade reference devices showed good performance of Respinos. Overall results demonstrate the potential of Respinos for remote patient monitoring during and post pandemic.

Index Terms—Vital signs, COVID-19, patient monitoring, spirometer, pulmonary diseases, mobile health.

I. INTRODUCTION

SINCE it was first identified in Wuhan, China, around December 2019, Coronavirus Disease 2019 (COVID-19) has continued to spread throughout the world. COVID-19,

This work was supported by the Indonesian Ministry of Research, Technology and Higher Education (Ristekdikti) under the Indonesian Collaborative Research Program (PPKI) grant (No. 542/IT1.B07.1/TA.00/2021). (*Corresponding author: Trio Adiono*).

Trio Adiono is with the School of Electrical Engineering and Informatics, Bandung Institute of Technology, 40132, Indonesia (e-mail: tadiono@stei.itb.ac.id).

Nur Ahmadi is with the Center for Artificial Intelligence (U-CoE AIVLB), School of Electrical Engineering and Informatics, Bandung Institute of Technology, Bandung, 40132, Indonesia (e-mail: nahmadi@itb.ac.id).

Citrya Saraswati, Yudi Aditya, Yusuf Purna Yudanto, and Abdillah Aziz are with Xirka, Bandung, Indonesia.

Laksmi Wulandari, Daniel Maranatha, Gemilang Khusnurrokhman and Agustinus Rizki Wirawan Riadi are with the Department of Pulmonology and Respiratory Medicine, Faculty of Medicine, Universitas Airlangga - RSUD dr. Soetomo, Surabaya, 60115, Indonesia.

Reza Widiyanto Sudjud is with the Faculty of Medicine, Universitas Padjadjaran, Sumedang, 45363, Indonesia.

which was officially declared as a pandemic by WHO on 11 March 2020 [1], has infected more than 480 million people and the death toll has reached more than 6.12 million people worldwide [2]. Cases of COVID-19 can be generally categorized as asymptomatic, mild, moderate, severe, and critical [3]. A recent study showed that 40.50% of confirmed COVID-19 population were asymptomatic [4] which indicates the potential risk of virus transmission from asymptomatic patients. Another study showed that among patients with symptoms, the proportion of them that had mild to moderate, severe, and critical illness were 81%, 14%, and 5%, respectively [5]. Highly contagious nature of COVID-19 has resulted in an excessive number of COVID-19 patients influx to the healthcare facilities. This has put an overwhelming burden to healthcare systems even in the developed countries like US and UK, which impacts the quality of care not only to COVID-19 patients but also to non-COVID-19 patients. To reduce the burden of healthcare system and prevent virus transmission, asymptomatic patients and patients with mild and moderate symptoms are recommended to self-isolate. However, the health condition of self-isolated patients may turn into severe or critical illness in a short period of time. Thus, it is of paramount importance to be able to monitor the vital sign parameters of self-isolated patients and give early warning if their health condition worsens [6]. The vital sign parameters that can be used as indicator of the progression of patients' health condition are shown in Table I. Most COVID-19 patients recover completely within a few weeks. However, for some people, the symptoms persist several weeks or months [7] — a condition referred to as “long COVID-19” or “post-COVID-19 syndrome”. The number of people experiencing long COVID-19 is unknown. According to a survey from the UK Government's Office for National Statistics in November 2020, it was estimated that 1 in 5 people had symptoms for more than 5 weeks and 1 in 10 people had symptoms beyond 12 weeks [8]. Long COVID-19 can affect multiple systems in the body including (not limited to) the respiratory and cardiovascular systems [9]. Therefore, a device capable of monitoring vital signs from not only self-isolated COVID-19 but also long COVID-19 patients and even non-COVID-19 patients is highly desirable.

In this paper, we propose a portable device that can monitor multiparameter vital signs of patients while undergoing self-isolation. We refer to the proposed device as Respinos. Respinos is equipped with a mobile application that can automatically analyze patient data and provide alarms and no-

TABLE I
PARAMETERS' VALUE FOR EARLY WARNING OF COVID-19 PATIENTS [10]

Parameters	Value	Unit
Respiratory rate (RR)	≥ 20	Breaths per minute (bpm)
Heart rate (HR)	≥ 100	Beats per minute (bpm)
Body temperature (T)	≥ 38	Degree Celcius ($^{\circ}\text{C}$)
Blood oxygen saturation (SpO ₂)	≤ 94	Percent (%)

tifications to the patient and clinician/medical staff if the health condition of patient is deteriorating. It minimizes interaction between patients and medical staffs which can reduce the risk of cross infections. In addition, it is also capable of performing spirometry to evaluate the lung function by measuring how much air a person can breathe out in one forced breath, which can provide objective information used in the diagnosis of lung diseases [11]. Respinos is not limited to COVID-19 patients; it can also be used to other patients that have lung problems, such as chronic obstructive pulmonary disease (COPD), cystic fibrosis (CF), asthma, and other pulmonary diseases [12], [13]. Therefore, it is suitable for the diagnosis and management of respiratory diseases patients and can be used to monitor patients during and post-pandemic.

The paper is organized as follows. Section II presents the related works, research gap, and summary of our contribution in the present work. Section III describes the system architecture including the operation mode, system specifications, and hardware block diagram. Section IV details the design of the proposed device from both the hardware and software perspectives. Section V explains the application system architecture comprising frontend and backend applications and its communication method. Lab and clinical trial data collection, system validation and analysis are presented and discussed in Section VI. Finally, conclusions are drawn in Section VII.

II. RELATED WORKS

The COVID-19 pandemic has accelerated the development and deployment of digital technologies for remote patient monitoring, which can include the use of portable/wearable devices, mobile and cloud applications, and IoT framework [10], [14]–[16]. Zhang and Ling proposed a telehealth monitoring system to monitor multiple physiological parameters including respiration rate (RR), heart rate (HR), body temperature, blood oxygen saturation (SpO₂), blood pressure, and electrocardiogram (ECG) [17]. It is connected to personal computer (PC) and mobile communication system module. Despite providing accurate measurement of multi-physiological parameters, it did not support mobile application which is more widely and easily accessible to general users. Raposo *et al.* developed a mobile health (mHealth) application and specialized device called e-CoVig for remote monitoring of vital signs (RR, HR, temperature, SpO₂, and cough) from patients during quarantine [18]. In another study [19], Taiwo and Ezugwu proposed a remote smart home healthcare support system (ShHeS) for monitoring vital signs such temperature, glucose level, and blood pressure. It incorporated multiple sensors, Android-based mobile phone, web application, and IoT connection.

Other studies addressed the remote monitoring problem using wearable tele-health system [3], [20], [21]. A pilot, proof of concept, observational study was conducted by Iqbal *et al.* by monitoring vital signs of suspected COVID-19 patients in the UK by using wearable patch sensor [22]. This study suggested the feasibility of wearable tele-health system for remote patient monitoring. Although the previously mentioned studies have the capability of monitoring multiple vital signs, they do not have the capability to test the lung function.

The lung function test is commonly conducted using a device called spirometer. There have been many studies reported in the literature on the design, development, and/or evaluation of spirometers. Rasyid *et al.* designed and developed portable spirometer connected to Android-based mobile application and web server [23]. However, it was not thoroughly validation against the standard reference device. Trivedy *et al.* designed and developed a low-cost, portable, smartphone-enabled spirometer with capability of classifying disease using a convolutional neural network (CNN) model [24]. Other studies focused on validation several commercially available portable spirometers [25]–[29]. Some examples of commercial portable spirometers are Spirobank Smart [30], Air Next [31], and alveoair [32]. Most of the existing spirometers do not support monitoring of vital signs such as HR, RR, temperature, and SpO₂. There are only few spirometers that support such feature, for example, Spirobank Oxi [33] and AioCare [34].

In this paper, we address the above problem by proposing a device that combines multiple vital signs measurement and lung function test. The contributions of this paper are as follows: 1) integration of multiparameter vital signs monitoring capabilities which are usually available on separate devices, 2) Support of remote and real-time monitoring capability via wireless connection to smartphone application and cloud data access. 3) UI/UX-based smartphone to reduce the device cost, form factor, and power consumption, 4) Nonlinearity compensation method of flow measurement with turbine-based spirometer, 5) Compensation method to eliminate the effect of inertia on the turbine which makes the turbine continue to rotate even though the exhalation has stopped, and 6) Compensation method for hand movements to improve the accuracy of SpO₂ measurement.

III. SYSTEM ARCHITECTURE

The system architecture of Respinos can be seen in Figure 1. It consists of a portable device that is used for breathing measurement through the mouthpiece. It wirelessly connects via bluetooth to a smartphone application which is connected to a database in the cloud. Thus, all measurement data can be observed in real-time by accessing data in the cloud with a computer or smartphone anytime and from anywhere. By breathing through the mouthpiece, Respinos can measure respiration rate and spirometry parameters: forced vital capacity (FVC), forced expiratory volume in the first second (FEV1), FEV1/FVC and peak expiratory flow rate (PEFR). It can also measure blood oxygen saturation (SpO₂) and heart rate through a finger-based photoplethysmogram (PPG) sensor. It is also equipped with a temperature sensor that is placed in

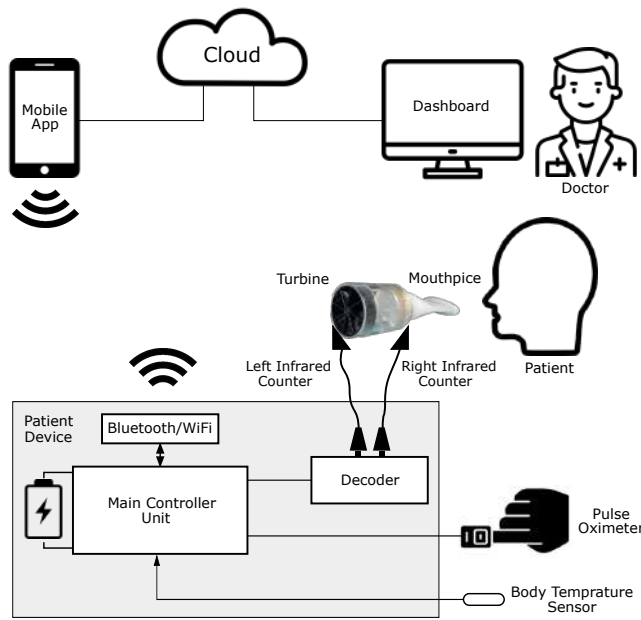


Fig. 1. System architecture of Respinos.

the armpit. It has two modes of operations, *monitoring mode* and *evaluation mode*, which will be explained in the following section.

A. Operation Mode

1) *Respiration Monitoring Mode*: In this mode, Respinos measures 4 parameters: RR, HR, body temperature, and SpO₂. The measurement results will be pushed to the cloud every 2 seconds. The patient is asked to breathe normally through the mouthpiece. Through the flow sensor connected to the mouthpiece, Respinos will detect when the patient inhales and exhales as seen in the normal breath section in Figure 2. The patient is considered to perform one breath if an inhalation is detected and followed by an exhalation. The average number of breaths detected in one minute is referred to as respiratory rate. To measure heart rate and SpO₂, Respinos uses a finger-based PPG sensor with DB25 connection as shown in Figure 3. To measure temperature, a thermistor sensor is used by inserting it into the patient's armpit.

2) *Spirometry Mode*: Spirometry is a physiological test that measures the maximal volume of air that an individual can inspire and expire with maximal effort [11]. In this mode, Respinos serves as a spirometer which measures the volume and the flow of breath. To carry out measurement, a patient has to perform maneuver of taking a deep breath and followed by blowing the air as hard as possible to the mouthpiece. The measurement results are stored in the form of flow-volume and volume-time curves. Using the measurement data, Respinos calculates and displays the curves of FVC, FEV₁, FEV₁/FVC, and PEFR.

The FVC is the volume delivered during an expiration by blowing the air as forcefully and completely as possible starting from deep inspiration. The FEV₁ is the expiratory volume in the first second of an FVC maneuver [11]. Patients can

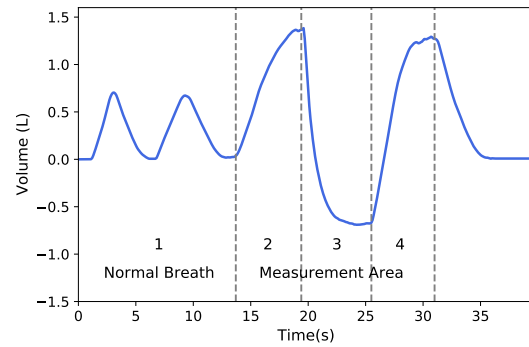


Fig. 2. Respiratory volume on spirometry test.



Fig. 3. Design of Respinos.

view a real-time graph of volume versus time on a smartphone application which can assist them by providing maneuvering directions. The test output is measured by the device when the patient's breath is in area 3 (see Figure 2). Especially for the F-V curve, the curve displays the data flow and volume from areas 3 and 4. Using this mode, Respinos can also detect pulmonary diseases, such as COPD, CF, and asthma. Several prototypes of spirometer developed and reported in literature can be seen in [23], [24], [35], [36].

B. System Specifications

The performance of Respinos is very dependent on its sensors' specifications, which are listed as follows:

1) Flow Sensor:

- Bi-directional digital turbine
- Flow range: ± 16 L/s
- Volume accuracy: $\pm 2.5\%$ or 0,05 L
- Flow accuracy: $\pm 5.0\%$ or 0,20 L/s
- Dynamic resistance: < 0.5 cm H₂O/L/s
- Sampling rate: 100Hz

2) Pulse Oximeter:

- SpO₂ range: 70% - 100%

3) Temperature Sensor:

- Temperature range: -55°C to $+125^{\circ}\text{C}$
- Temperature accuracy: $\pm 0.5^{\circ}$ from -10°C to $+85^{\circ}\text{C}$

4) Peripherals and Interfaces:

- 802.11b/g/n HT40 Wi-Fi transceiver
- Micro USB connector for charging
- Battery : 800 mAh
- LED status

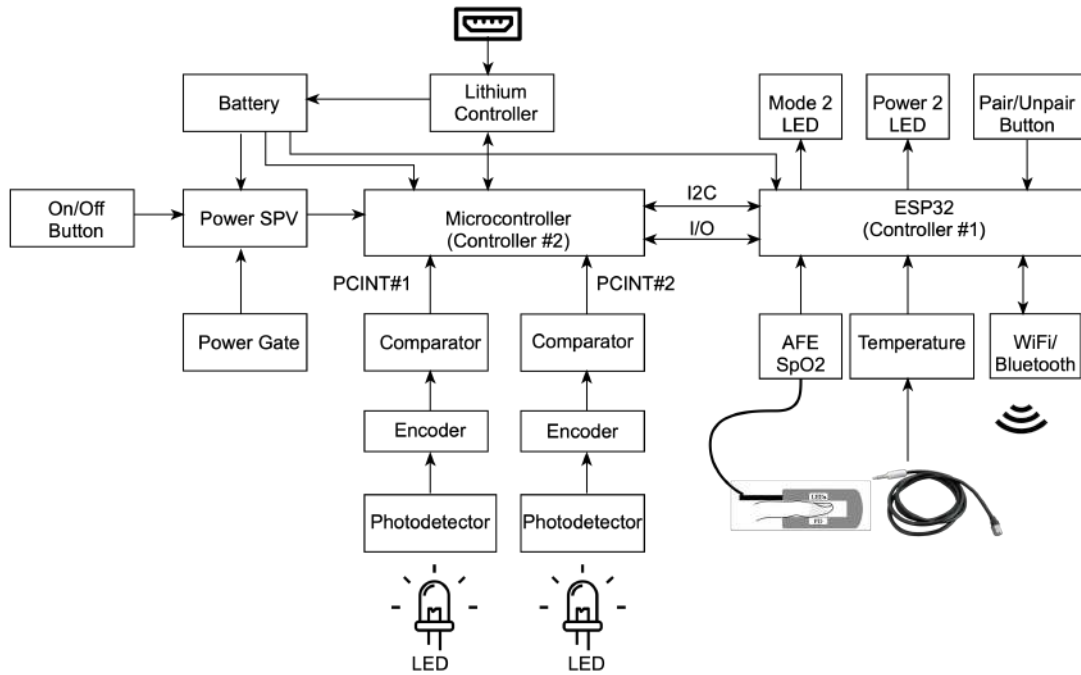


Fig. 4. Hardware block diagram of Respinos.

C. Hardware Block Diagram

The hardware block diagram of Respinos is shown in Figure 4. It has three sensors to measure vital signs, which are turbine, PPG and temperature sensor. The bidirectional turbine with rotary sensors is used to measure the patient's breathing conditions. The turbine is connected to two left and right infrared counter. It measures the flow velocity and direction using decoder. From velocity and direction parameters, RR and other lung condition parameters can be measured. The decoder is connected to a main control unit through general-purpose input/output (GPIO) port. To prevent spread of virus transmission between users, disposable mouthpiece is used in front of the turbine. The PPG sensor measures SpO2 and HR through sensing patient's blood volume changes in the microvascular bed of tissue. This sensor is also connected through serial port of the main control unit. The whole signal processing and control functions are carried out by the main control unit.

Respinos has an external communication module in the form of bluetooth or WiFi which enables wireless connection to a smartphone application. The smartphone application has three main functions, namely displaying measurement data, giving alarms in case of abnormal conditions, and sending data to the cloud. Data from Respinos are connected to the data center in the cloud in real-time. The data in the cloud can thus be accessed by medical staff to monitor the patient's condition. The cloud data center is also equipped with data analytics. For optimal quality control, both volume-time and flow-volume real-time displays are required, and operators must visually inspect the performance of each maneuver for quality assurance before proceeding with another maneuver [11].

IV. DEVICE DESIGN

A. Hardware Design

The hardware block diagram of Respinos is shown in Figure 4. It consists of the main control unit, sensors, battery and communication. It has a main sensor in the form of a flow disposable turbine. This turbine measures flow velocity and volume of breath based turbine rotation due to breath. The turbine rotation is detected through infrared sensors. For the temperature sensor, the DS18B20 digital thermometer is used [37]. For the communication, an ESP32 chip is used which has WiFi and bluetooth connections [38]. For SpO2 measurement, we use the AFE4400 integrated analog front-end [39]. Respinos has two control units, the first is a 32-bit microcontroller that is integrated with WiFi module using the ESP32 component; the second is an 8-bit microcontroller using an ATmega component. The first microcontroller serves as the main computing unit, whereas the second microcontroller is used to convert the pulse from the turbine into an uncompensated flow. Breathing flow is calculated through the number of turbine rotations which are detected through the LED signal that arrives at the photodetector. The photodetector analog signal is converted into a digital signal using a comparator module. We use a threshold of <0.37 V as low data and >0.57 V as high data. The comparator output is connected to the interrupt pin (PCINT#1 and PCINT#2) of microcontroller #2 to be translated as flow. The calculated flow in microcontroller #2 is sent to microcontroller #1 via the I2C interface for further processing.

Respinos uses a rechargeable 800 mAh lithium battery as a power supply. As the average power consumption of the appliance is 200 mA, it is expected to be used continuously for about 4 hours. This amount is sufficient to support the

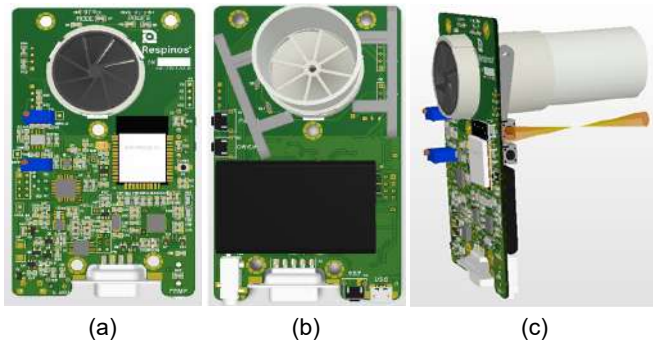


Fig. 5. Design of Respinos viewed from (a) top, (b) bottom, and (c) side.

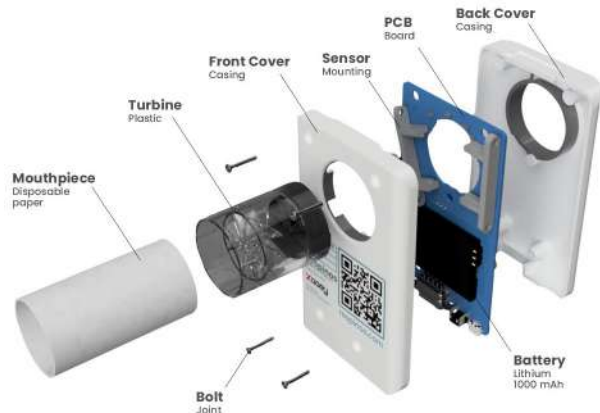


Fig. 6. The component breakdown of Respinos.

monitoring and spirometer modes. To control the power consumption, the power SPV module [40] is used that will always be on with very low frequency and power consumption. It manages the power gate module which will set all module into on and off based on the button switch state. Respinos has four LED indicators: PWR0, PWR1, MODE0 and MODE1. PWR0 turns on when the device is on and not low battery; PWR1 is on/off when device is low battery; MODE0 turns on when bluetooth/WiFi is connected and idle; MODE1 is on in spirometry mode, and on and off in basic mode. The top and bottom views of Respinos design are shown in Figure 5(a)-(b). The turbine is placed on the top. At the bottom, there are two connection ports to the PPG and temperature sensors. The WiFi module is placed on the surface. The side view of Respinos design can be seen in Figure 5(c). The component breakdown of Respinos is illustrated in Figure 6. The 800 mAh battery size is relatively small, so the device can still be used as a hand held,

The primary reason why turbine spirometer was selected because it does not require frequent calibrations and have comparable accuracy to those of conventional spirometers [41]–[43]. Turbine spirometers are suitable for portable applications, especially when the trend value is more important than absolute value. In addition, turbine spirometers are relatively insensitive to gas composition, humidity and altitude, and its rotation is linear with respect to its speed and air flow [44]. The turbine can work bidirectional and detect inhale and exhale activities easily. Turbine measurement performance is not affected by the temperature and pressure variations [45]. One of the novelties of this paper is the method for overcoming the moment of inertia, namely the problem of still rotating the turbine even though the breath has stopped, and also the problem of moving the inhale to the exhale and vice versa. This feature is very important to determine the end of expiration.

B. Software Design

1) *Flow Detection*: The mechanism of respiratory flow detection in the spirometer function is illustrated in Figure 7. The air flow entering the turbine will be directed by a deflector so that the air flow rotates. This rotating airflow causes the flat blades of the turbine to rotate. Turbine rotation is detected by 2 pairs of LEDs and phototransistor. The LED

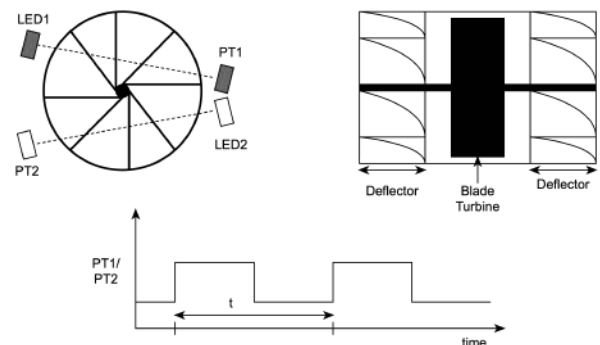


Fig. 7. Flow detection mechanism.

and phototransistor1 (PT1) are positioned so that when the turbine blade moves, the light from the LED will be detected and PT1 will not be detected alternately, so that the signal from PT1 forms a pulse.

The microcontroller increases the counter count every $16 \mu s$. When a rising edge is detected in the PT1 pulse, the counter value of t is read and stored as a period. From this t value, the frequency (f) of turbine blade rotation can be obtained. The relationship between air flow (Q) and frequency (f) is formulated as:

$$Q = kf \quad (1)$$

The value of k was determined empirically through experiments. The relationship between the turbine rotation and flow is shown in Figure 8(a).

The relationship between the turbine rotation speed and flow is not always linear, especially at low flows. This effect is called the static flow effect [46]. For this reason, a compensation process is required and implemented using following mechanism. We call the uncompensated flow as Q and the compensated flow due to static effect as Q_{st} . A commercial digital flow sensor from Sensirion SFM3000-200 [47] was used as reference whose measured data is denoted as Q_s . The comparison of Q with Q_s does not always show a value of 1 as shown in Figure 8(b).

By using a solver, we obtain the equation of k as a function

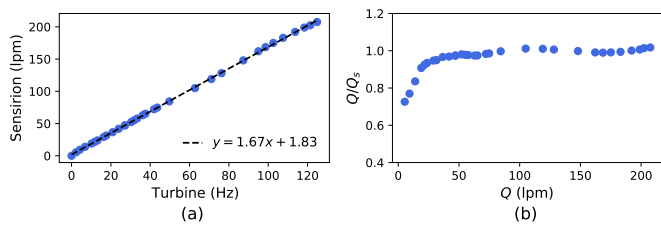


Fig. 8. Turbine rotation and flow. (a) The correlation between turbine rotation and flow. (b) Uncompensated flow Q vs. reference flow Q_s .

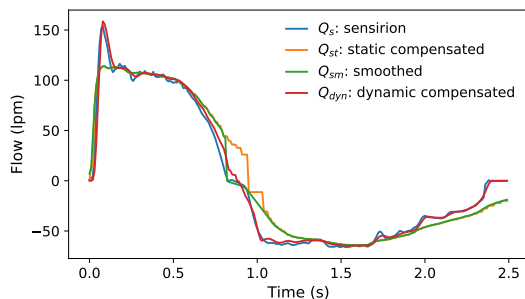


Fig. 9. Dynamic compensated turbine generated flow Q_{dyn} versus reference flow Q_s (Sensirion) and static compensated of measured turbine generated flow Q_{st} .

of turbine frequency in Hz as shown in Eq. (2).

$$k(x) = 1.67x + 1.83 \quad (2)$$

Using this compensation equation, we can calculate the static compensated flow Q_{st} in Eq. (3).

$$Q_{st} = Q \times k(x) \quad (3)$$

Since we sample the data with period of 0.01 second (100 Hz), if the flow is less than 100 LPM, the sample is less than time period. Therefore, we need to interpolate the Q_{st} data using interpolation filter function F as defined in Eq. (4) to obtain smoothed graph (Q_{sm}).

$$Q_{sm} = F(Q_{st}) \quad (4)$$

The static compensated flow Q_{st} and smoothed data Q_{sm} results are shown in Figure 9. Due to inertia of turbine, we need to compensate the flow with dynamic compensation factor. The dynamic compensated flow, denoted as Q_{dyn} , can be defined in Eq. (5) [46].

$$Q_{dyn} = Q_{sm} \times \left(1 + \tau \frac{df}{dt}\right) \quad (5)$$

The $\frac{df}{dt}$ is the speed of the flow change and τ is the value to compensate the dynamic flow. To determine the value of τ , we conducted an experiment by spirometry maneuver (inhale and exhale) and compared the measurement results between turbine generated flow Q_{st} and a reference digital sensor (Sensirion), Q_s with sampling period of 10 ms is shown in Figure 9. It is shown that there are large differences between Q_{st} and Q_s at the start, middle and end area. At low flow, a higher τ value is required. On the contrary, at high flow, a lower τ value is required. It can be seen that there is a

TABLE II
THRESHOLD (THD) VALUE FOR STOP INDICATOR

Flow (LPM)	Threshold (THD)
15 - 300	0.119
> 300	0.32
< 15	0.08

correlation between flow and τ value. The τ factor changes dynamically and is not fixed. In order to approximate the reference flow, we apply several processing.

Through a series of experiments, we found the appropriate τ value as shown in Eq. (6).

$$\tau = \left(\frac{100}{Q}\right)^{1.75} \times 0.33 \quad (6)$$

As a result, we can see that the dynamic compensated flow Q_{dyn} is almost overlapped with the reference flow Q_s (see Figure 9). The constant k in Eq. (2) changes slightly for different mouth pieces and turbines even though they are of the same type and company. Changes can be corrected by adjusting the constant k at the time of calibration using a calibration syringe as reference. For the τ value, according to our experiments, it does not change much for the mouth piece and turbine of the same type.

Detecting that the flow source has completely stopped is difficult because the turbine has an inertial property. Even though the patient has stopped breathing, due to the inertia of the turbine, the turbine blades are still rotating. To detect this, we propose the following method. The flow is measured periodically. If there is a change in the period greater than a certain threshold value (THD), it is assumed that the flow stops. This THD value is different for different flow ranges. The THD value was determined through a series of experiments. Experiments were carried out using a flow source from a calibration syringe. As a flow reference, a digital flow sensor was used [47]. From the experimental results, we obtained the appropriate THD value as shown in Table II. Using this approach, the flow stops although the turbine is still rotating due to inertia.

2) *Breath count detection*: The process of detecting the number of breaths is calculated based on the measured flow value. The direction of positive or negative flow is known from the phase difference between phototransistor 1 and 2. For positive flow, the pulse value of PT2 on the rising edge of PT1 is high. Conversely, when the flow is negative, the pulse value of PT2 on the rising edge of PT1 is low (see Figure 10). To detect whether the breath is inhaled or exhaled, it can be done by detecting the direction of rotation.

The respiratory rate measurement process is performed using a flowchart as shown in Figure 11. Measurement starts when the start button is activated. Next, the inhale detection process is carried out through the flow value > 0 . At this time, the measurement time starts. Furthermore, the detection of exhale is when there is a change in flow < 0 . Next is to re-detect inhale through flow > 0 . When this occurs, a complete breath cycle has been measured. Measurement errors can occur due to sensor errors or incorrect use of tools. For this reason,

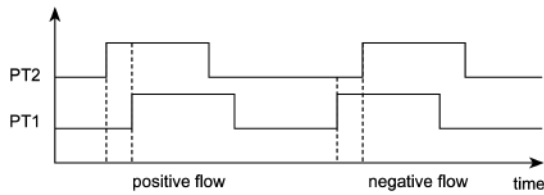


Fig. 10. Positive and negative flow detection.

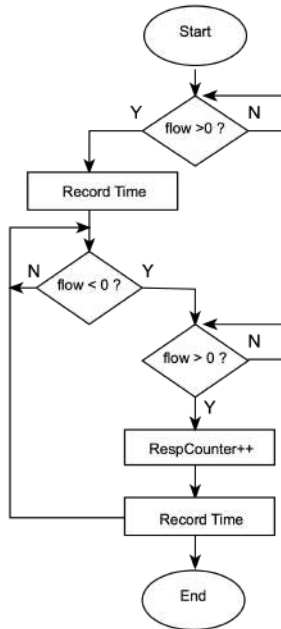


Fig. 11. Respiratory rate measurement flowchart.

a 20 second moving average respiratory rate is employed. The respiratory rate is calculated after each complete breath cycle. One breath cycle begins with inspiration and ends with expiration. The update process is done every 5 seconds. Therefore, 5 seconds are from new data and 15 seconds are from the previous data.

3) *Spirometry Measurement:* The spirometry measurement flowchart is shown in Figure 12. Measurement starts when the start button is activated. Next, the device waits until an inspiratory maneuver is detected which is indicated by $flow > 0$. Then, the device waits until an expiratory maneuver occurs which is indicated by $flow < 0$. In this state, the device will measure and record the volume value to get the spirometry parameter value. This process will be completed when the stop button is activated. Otherwise, if the expiration is complete and the maneuver continues to inspiration ($flow > 0$), then the data will be recorded for display, but does not include the data used in the measurement.

From the flow recording, spirometry parameters are calculated as shown in Figure 13. FVC is calculated from the maximum volume that occurs. FEV1 is a volume value calculated 1 second from the start point. PEFR is calculated from the maximum existing flow. Finally, FEV1/FVC is calculated from the previously measured FEV1 and FVC parameters.

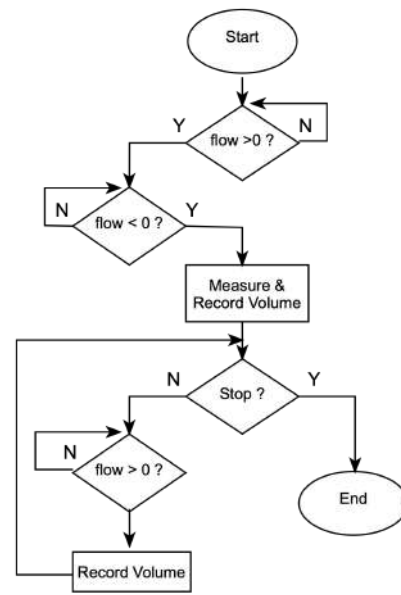


Fig. 12. Spirometry measurement flowchart.

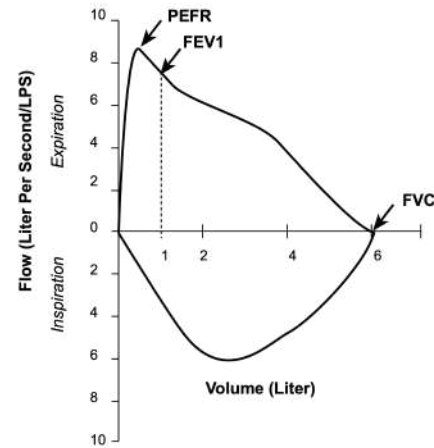


Fig. 13. Spirometry curve and parameters.

4) *SpO2 Measurement:* The SpO2 measurement process was carried out using two signals, namely red (R) and infrared (IR) using sensor which was placed on the finger. These two signals are generated by different LEDs and each is sensed by a photodetector. The signals consist of AC and DC components. The AC component is influenced by changes in blood vessels during systole and diastole. The blood in vessel absorbs the light intensity, thus reducing the light intensity which is either transmitted or back-scattered. The detected signal in photodetector is correlated with the concentration of oxygen in the blood. Meanwhile, the DC component correlates with venous blood, skin and tissue. In order to eliminate the effect of the variant of absorbance due to venous blood condition and surrounding tissues, we normalized the R and IR signals with their respective DC values as shown in Eq. (7).

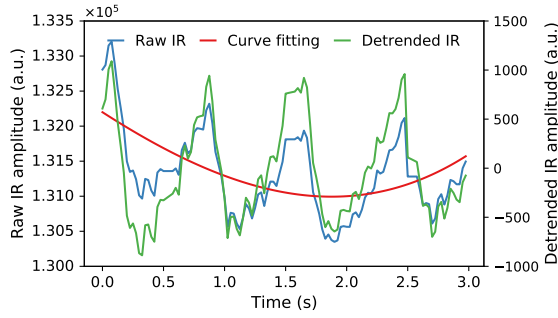


Fig. 14. Finger movement compensation.

$$\frac{R}{IR} = \left(\frac{AC_R}{DC_R} / \frac{AC_{IR}}{DC_{IR}} \right) \quad (7)$$

The ratio of R/IR is correlated with SpO2 [48]. When the ratio is 1, the SpO2 value is about 85%. Therefore, the estimation of SaO2 using the empirical relationship can be given in Eq. (8).

$$SaO2(\%) = A - B \cdot (R/IR) \quad (8)$$

However, during measurement, finger motion artifact can affect the measurement results as shown in “raw infrared” graph in Figure 14. This measured raw data denoted as M . In order to stabilize the signal, we detected basic motion artifact caused by respiration, sympathetic nervous system and thermoregulation as shown in “curve fitting” graph in Figure 14 with sampling rate of 40 Hz. Using the equation of detected finger movement graph, denoted by $f(x)$, we can compensate the finger movement using polynomial curve fitting (PCF) method with fourth order, which can be formulated in Eq. (9). The result of compensated signal, denoted by M' , is shown in Figure 14 (see detrended IR).

$$M' = M - f(x) \quad (9)$$

5) *HR Measurement*: HR is calculated by detecting the peak of infrared signal and measuring its period. The detail method to calculate the HR is illustrated in Figure 15. The peak is detected when the current value of infrared, denoted by IR , is lower than the previous value. If this remains true for 0.125 s, then a peak is acquired. We call this state ($peakAcq$) as True. While a peak is not acquired, we save the current value to a variable called $peakIR$, and save the current time to a variable called $beatTime$. To eliminate peak caused by diastolic peak, any peak that is lower than half of the last peak value is discarded. The last peak value and time are saved to $last_peakIR$ and $last_beatTime$ variables, respectively. The time between the previous peak and current peak is saved to a circular array. Its median is used to calculate the heart rate.

V. APPLICATION SYSTEM ARCHITECTURE

The application system architecture of Respinos involves several components: Respinos device, user application, backend service, database service, and message broker service as illustrated in Figure 16. User can scan and control active

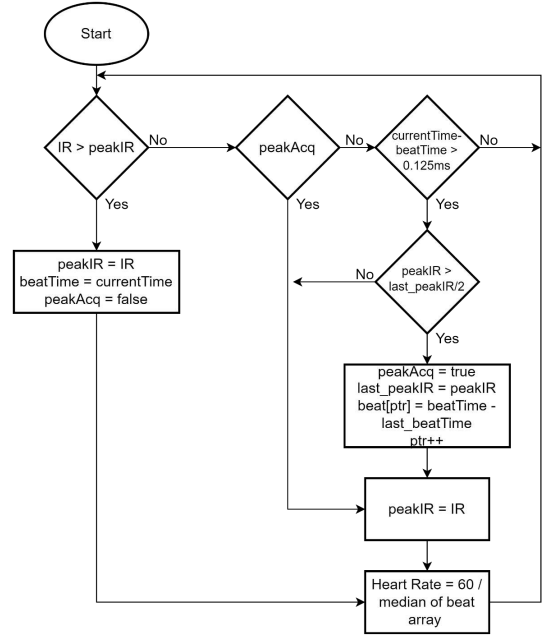


Fig. 15. Heart Rate (HR) measurement method.

Respinos device through the smartphone application. After selecting the active device, patient and measurement mode, the user can start the measurement. Device control is carried out on top of the bluetooth protocol. The measurement execution message received by the device initiates the measurement and transmits the measurement results via the same protocol. Measurement result data is displayed in the smartphone application in the form of numbers or graphs in real-time.

If the smartphone application is connected to the internet, it will send the measurement results through the message queuing telemetry transport (MQTT) protocol [49] via a message broker. The message broker receives the measurement data, then passes it on to other clients who need this information. With this scheme, other applications (e.g. smartphone or web applications) can receive/display the information in real-time. After the measurement is stopped, the smartphone device sends all the measurement data results to the backend service to be stored in the database. All medical record information can be accessed anytime and anywhere by doctors via the smartphone or web applications.

A. Respinos Device

Respinos device is a hardware device whose role is to receive and execute commands from the user through the application, perform measurements and send measurement results to the application.

B. User Application

User application consists of smartphone and web based applications that act as user interface services. Smartphone application can control the device functions and show its measurement data. The web based application can access the measurement information through backend/message broker

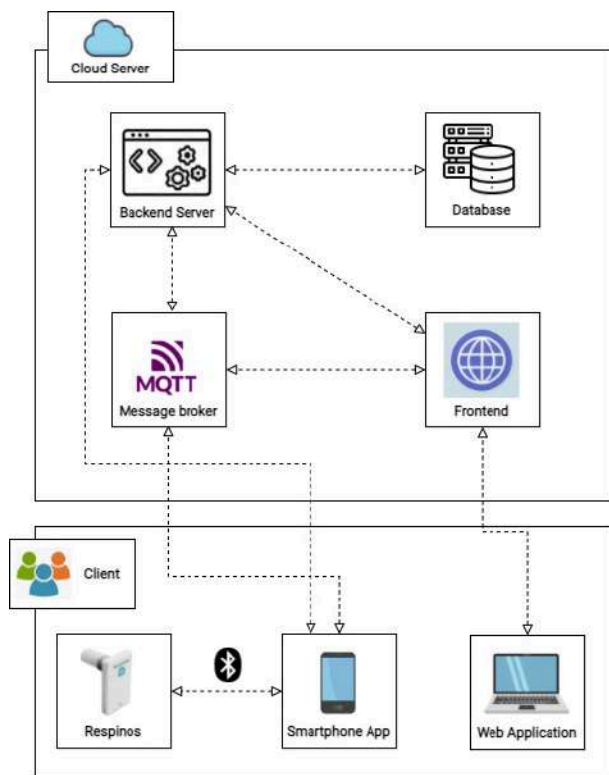


Fig. 16. The application system architecture of Respinos.

services. Users who can access this service are verified users via the login page in the application. The UI/UX of application is shown in Figure 17. Using the application of monitoring mode, we can monitor temperature, SpO2, RR and HR in real-time. On the other hand, we can monitor the lung condition using the application spirometer mode. In spirometer mode, we can see the parameter of FVC, FEV1, PEF and ratio, including its flow vs. volume curve. We also display the estimated normal value based on age calculation. The application has two communications which are via Web API and MQTT Broker.

1) *Communication with Web API*: The application gets and sends data such as patient details, changes to patient data or patient records via a web application programming interface (API). The Web API accepts hypertext transfer protocol (HTTP) requests such as GET, POST, PATCH and DELETE and then sends an HTTP response in response. Response data from the web API is included in JavaScript Object Notation (JSON) [50], which will be processed by the native app. The native app also sends commands to start and stop the Respinos device via the web API. The JSON format for respiration monitoring mode is as follows:

```
{payload:{SPO2: {#}, RR: {#}, T: {#}, HR: {#}}}
```

The detail parameter description can be seen in Table III.

The JSON format for spirometry mode is as follows:

```
{"value": {
  "FVC": {#},
  "FEV1": {#},
  "PEF": {#},
  "ratio": {#},
  "TimeSeriesLength": {#},
```

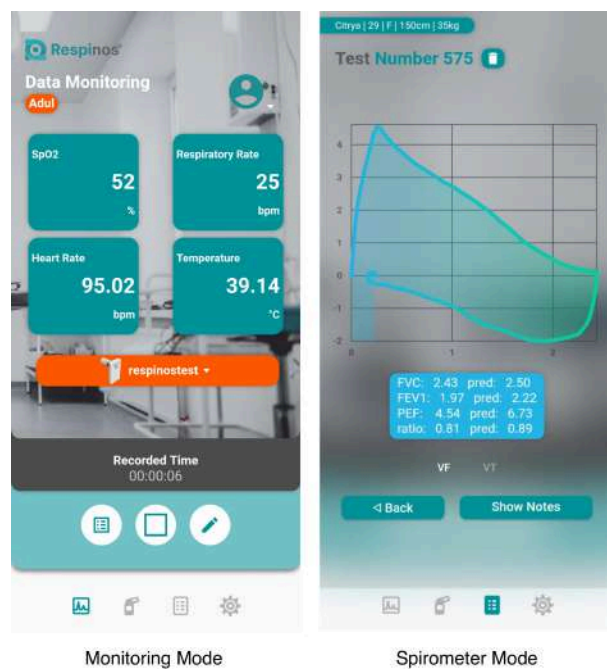


Fig. 17. The UI/UX of the main application.

TABLE III
JSON FORMAT PARAMETER DATA FOR MONITORING MODE

Parameter	Data Type	Unit
Respiratory Rate (RR)	int	bpm
Heart rate (HR)	int	bpm
Body temperature (T)	float	°C
Blood oxygen saturation (SpO2)	int	%

TABLE IV
JSON FORMAT PARAMETER DATA FOR SPIROMETRY MODE.

Parameter	Data Type	Unit	Description
value	object		Parameters of the measurement results
FVC	float	L	Forced vital capacity
FEV1	float	L	First expiratory volume in 1st second
PEF	float	L/s	Peak expiratory flow
ratio	int		Ratio of FEV1/FVC
TimeSeriesLength	int		Timeseries graph array length
XYLength	int		Graph XY array length
graph	object		Array of measurement result curve
timeseries	array	L	Volume vs. time curve during expiration
XY	array	[L,L/s]	Flow to volume curve

```
    "XYLength": {#}
  },
  "graph": {
    "timeseries": [{#},{#},...],
    "XY": [
      [{#}, {#}],
      [{#}, {#}],
      ...
    ]
  }
}
```

The detail parameter description can be seen in Table IV.

2) *Communication with MQTT Broker*: The app also communicates with the MQTT broker to get the state of the device. It is used to check whether the device is off or on. If the app is

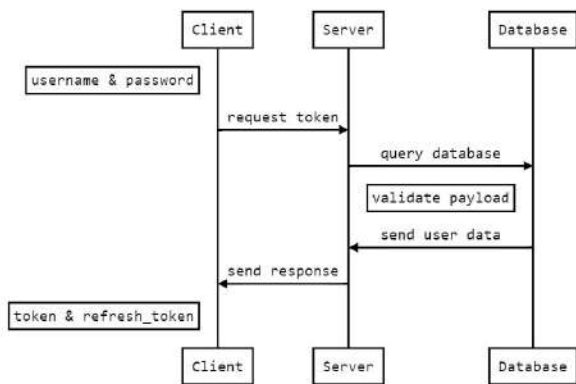


Fig. 18. Token acquisition scheme via server.

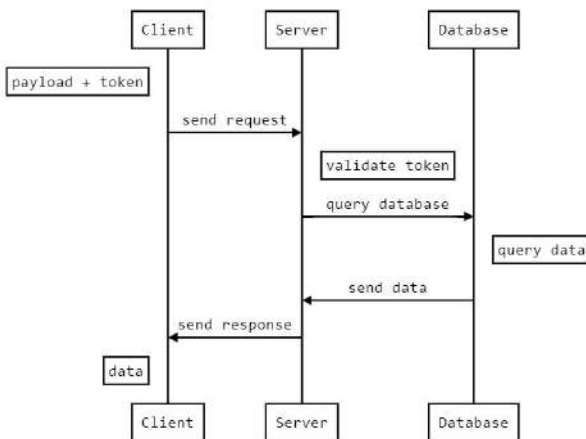


Fig. 19. Data request scheme from client through server.

detected with WiFi but cannot get the state of the device, the user will be asked to set WiFi. The data sent from the device in the form of JSON is also obtained from the broker.

C. Backend Service

Backend service is a web service whose role is to access or manipulate data from the database requested by the client. This service applies the RESTful API architectural style [51] which uses the HTTP protocol to make requests by clients. To maintain data security, clients requesting data through this service will be checked for authentication and authorization through a token verification scheme. This token is obtained when the client logs in to the application. The token request process is illustrated in Figure 18. The data exchange between client and server using the token is illustrated in Figure 19.

D. Database service

The data is stored in a database system installed in the cloud. This data storage service can only be accessed through the backend service. The database system software used is MongoDB [52]. Collections of data stored in the database include the following:

- 1) User: a collection containing user documents

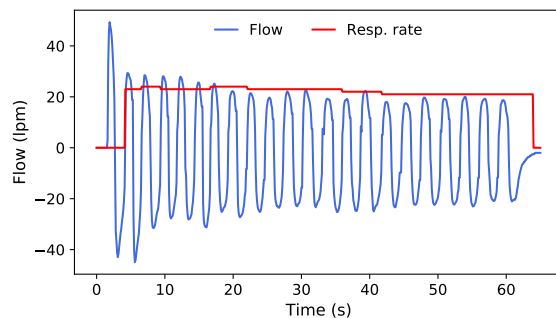


Fig. 20. Flow waveform and respiration rate measurement from Respinos.

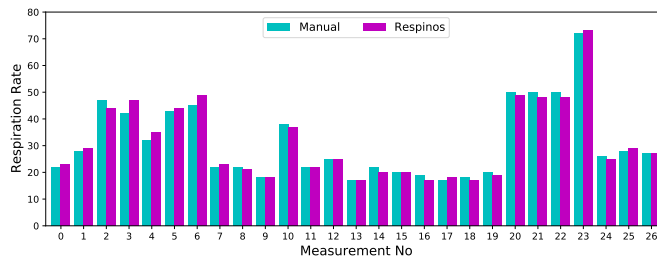


Fig. 21. Comparison between Respinos and measurements.

- 2) Device: a collection containing Respinos device information
- 3) Patient: a collection containing patient information
- 4) Record: a collection that contains information on medical records/patient measurement results using a Respinos device

E. Message broker service

Message exchange service using the MQTT protocol. To implement the message broker service, open source-based software is used, namely Mosquitto [53]. By using this service, clients can send real-time information to other clients. Some of its implementations on this system are sending measurement results and notification of data changes to clients.

VI. RESULTS AND DISCUSSION

A. Evaluation of Respiration Measurements

Respiration measurements were conducted by patients through breathing normally on the mouthpiece of Respinos. Respinos recorded the respiratory flow as shown in Figure 20. The measurement results were compared against manual measurements which refers to the patient's breathing measured manually through physical appearance. The comparison results between Respinos and manual measurements are shown in Figure 21. The mean absolute error (MAE) was used as performance metric and calculated as the absolute difference between Respinos and manual measurements. Across 27 measurements, we found an MAE of 1.33 ± 1.24 , which demonstrates good accuracy of Respinos.

TABLE V
MEASUREMENT OF SPO₂ AND HR WITH SETTING OF 2% PULSE AMPLITUDE, MEDIUM FINGER, AND NO ARTIFACT.

HR Setting	30 bpm		60 bpm		120 bpm		180 bpm	
SpO ₂ Setting	SpO ₂ (%)	HR (bpm)	SpO ₂ (%)	HR (bpm)	SpO ₂ (%)	HR (bpm)	SpO ₂ (%)	HR (bpm)
99	99	30	99	60	99	120	99	180.72
98	98	30	98	60	98	120	98	180.54
97	97	30	97	60	97	120	97	181.75
95	95	30	95	60	95	120	95	180.98
90	90	30	90	60	90	120	89.92	180.33
85	85	30	85	60	85	120	85	180.17
80	80	30	80	60	80	120	79.97	180.64
70	70	30	70	60	69.95	120	70	180.99

TABLE VI
MEASUREMENT OF SPO₂ AND HR WITH SETTING OF 10% PULSE AMPLITUDE, SMALL FINGER, AND 2.5% RESPIRATION ARTIFACT.

HR Setting	30 bpm		60 bpm		120 bpm		180 bpm	
SpO ₂ Setting	SpO ₂ (%)	HR (bpm)	SpO ₂ (%)	HR (bpm)	SpO ₂ (%)	HR (bpm)	SpO ₂ (%)	HR (bpm)
99	99	30	99	60	99	120	99	181.08
98	98	30	98	60	98	120	98	181.35
97	97	30	97	60	97	120	97	181.16
95	95	30	95	60	95	120	95	181.11
90	90	30	90	60	90	120	90	180.57
85	85	30	85	60	85	120	85	181.44
80	80	30	80	60	80	120	80	180.53
70	70	30	70	60	70	120	70	181.66

B. Evaluation of SpO₂ and HR Measurements

SpO₂ measurements were carried out simultaneously with HR measurements because it used the same PPG sensor. The measurements were compared against an industrial standard measuring instrument, which is ProSim SPOT Light SpO₂ Pulse Oximeter Tester (Fluke Biomedical, US) [54]. The comparison were made by varying the SpO₂ and HR values generated by the instrument through the PPG sensor. We used three settings : 1) 2% pulse amplitude, medium finger, and no artifact; 2) 10% pulse amplitude, small finger, and 2.5% respiration artifact; 3) 2% pulse amplitude, large finger, and 2.5% respiration artifact. The ideal condition was represented by setting 1. The value of 2% is a good general value so that the signal is easy to detect from the signal range of 0.5% to 10%. In setting 2, the testing was carried out under extreme conditions, where the amplitude was set to maximum (10%). The objective was to test Respinos under the maximum input. Therefore, we could observe if the overflow was detected. We also tested Respinos using small finger with 2.5% artifact from respiration. The measurement results from setting 1, 2, and 3 are shown in Tables V, VI, VII, respectively. Tables V-VII show that Respinos' SpO₂ and HR measurements are accurate as reflected by small error (<1) between Respinos' the reference's results.

C. Evaluation of Temperature Measurements

Temperature measurements were evaluated by comparing Respinos with with Fluke 88V Deluxe Automotive Multimeter

TABLE VII
MEASUREMENT OF SPO₂ AND HR WITH SETTING OF 2% PULSE AMPLITUDE, LARGE FINGER, AND 2.5% RESPIRATION ARTIFACT.

HR Setting	30 bpm		60 bpm		120 bpm		180 bpm	
SpO ₂ Setting	SpO ₂ (%)	HR (bpm)	SpO ₂ (%)	HR (bpm)	SpO ₂ (%)	HR (bpm)	SpO ₂ (%)	HR (bpm)
99	99	30	99	60	99	120	99	180.32
98	98	30	98	60	98	120	98	179.61
97	97	30	97	60	97	120	97	180.60
95	95	30	95	60	95	120	95	180.91
90	90	30	90	60	90	120	90	180.67
85	85	30	85	59.96	85	120	85	180.78
80	79.84	30	79.93	60	80	120	80	179.82
70	69.39	30	69.36	59.94	69.43	119.82	69.26	179.80

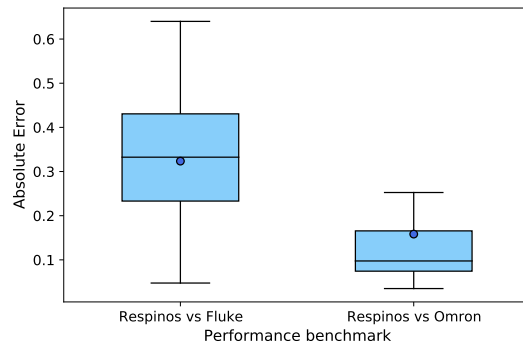


Fig. 22. Temperature measurement error.

TABLE VIII
INHALED VOLUME MEASUREMENT ERROR.

Volume Setting (L)	Inhaled Volume					Average Error (%)
	Fast (L)	Slow (L)	Fast, Slow End (L)	Slow, Fast End (L)		
0.5	0.52	0.39	0.48	0.45		8.00
1.0	1.01	0.88	0.90	0.97		6.00
1.5	1.54	1.44	1.46	1.57		0.17
2.0	2.07	1.96	2.03	1.99		0.62
2.5	2.59	2.43	2.53	2.5		0.50
Average Error (%)	2.95	8.56	3.87	3.63		3.06

(Fluke Biomedical, US) [55] as first reference and Omron Digital Thermometer MC-343F (Omron Healthcare, Indonesia) [56] as second reference. The measurement results can be seen in Figure 22. It can be seen that Respinos' results are close to the reference devices' results. The mean absolute error (MAE) and mean absolute percentage error (MAPE) of Respinos with respect to the Fluke were 0.32 ± 0.16 and $0.93\% \pm 0.47\%$, respectively. The MAE and MAPE of Respinos with respect to the Omron were 0.16 ± 0.14 and $0.45\% \pm 0.14\%$, respectively.

D. Evaluation of Volume Measurements

Experiments were conducted to test how accurately Respinos can measure volume by using standardized equipment (BTL 3L calibration volume syringe) that can generate a certain volume of air. In these experiments, the volumes generated were in the lung volume range (0.5, 1.0, 1.5, 2.0,

TABLE IX
EXHALED VOLUME MEASUREMENT ERROR.

Volume Setting (L)	Exhaled Volume				
	Fast (L)	Slow (L)	Fast, Slow End (L)	Slow, Fast End (L)	Average Error (%)
0.5	0.44	0.42	0.47	0.38	14.50
1.0	0.95	0.87	0.91	0.92	8.75
1.5	1.44	1.48	1.40	1.41	4.50
2.0	1.97	1.92	1.98	1.93	2.50
2.5	2.43	2.49	2.49	2.39	2.00
Average Error (%)	5.06	6.95	4.61	9.18	6.45

and 2.5) as shown in Table VIII and Table IX. In addition to changing the volume, speed was also varied to measure changes in accuracy with time. This was to resemble the actual condition of the patient, where the ability to inhale and exhale varies between people. The main variations of volume with time were fast and slow. However, to make it more equal, variations of changes from fast to slow were also made and vice versa. As shown in Table VIII, although there were large error in few measurements, the overall average error was relatively low (3.06%). The large error occurred in measurements with small volumes, especially at slow speeds. The largest percentage of errors occurs in measurements at low speeds, which reached 8.56%. On the other hand, the highest percentage of error with respect to speed was in fast measurements.

Similar results were also observed in the case of exhale measurements as shown in Table IX. The largest error occurred in measurements with small volumes (0.5 liters), which reached 14.5%. The measurement on this volume that was not accurate was the slow to fast measurement with an error of 9.18%. In general, the exhale error was higher (6.45%) compared to that of inhale (3.06%).

E. Evaluation of Spirometer Parameter Measurements

To evaluate the performance of Respinos for measuring spirometer parameters, experiments were carried out on an adult aged 32 years old with a height of 165 cm. Four spirometer parameters (FVC, FEV1, FEV1/FVC, and PEFr) were measured and compared against a medical-grade reference device: Contec SP80B spirometer (Contec Medical Systems, China) [57]. The performance comparison between Respinos and the reference for FVC, FEV1, FEV1/FVC, and PEFr are shown in Table X.

We found that the average error of FVC measurements between Respinos and the reference was 0.51% with maximum error of 2.00%. In the FEV1 measurements, the average error was 1.76% with maximum error of 4.10%. In the case of FEV1/FVC measurements, the average and maximum errors were 2.55% and 3.65%, respectively. For PEFr measurements, Respinos yielded an average error of 2.53% and maximum error of 4.21%. These measurement errors are small which indicate that Respinos performs well. Parameters FEV1 and FVC vary with age, height, gender and ethnicity. Interpretation of spirometry requires comparison of the patient's measured

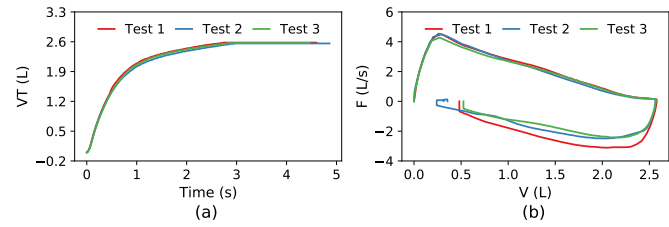


Fig. 23. Spirometry test result using Respinos from three tests. (a) Vt-time plot. (b) F-V plot.

values (FVC, FEV1, %FEV1-FVC1 ratio) with expected values obtained from predictor equations [45]. Examples of spirometry's measured values and expected values from three tests are shown in Table XI. Examples of tidal volume vs. time (VT-time) and flow vs. volume (F-V) graphs from three tests are shown in Figure 23.

F. Clinical Trial

The clinical trial was reviewed and approved by Ethical Committee in Health Research of Dr. Soetomo General Hospital, Surabaya, Indonesia (0239/KEPK/VIII/2021). Each subject was informed about the study and provided written informed consent. After the subjects signed the consent form to participate in the study, the subjects would receive a Respinos device to be used to monitor their condition for 6 days, in accordance with the direction of the health worker. Monitoring of vital signs was carried out 3 times (morning, afternoon, and night) for the first 5 days and 1 time (morning) in the sixth day. This result in 60 measurements per subject across 6 days. The clinical trial focused on monitoring 4 vital signs: RR, HR, body temperature, and SpO2. Temperature measurements were compared against Microlife MT 200 Digital Thermometer [58], whereas RR, HR, and SpO2 measurements were compared against Patient Monitor Mindray Beneview T8 [59].

Data collection in this study was carried out in October – November 2021. There were 97 subjects who met the inclusion criteria and had given informed consent to participate in this study. No subjects were excluded from this study. The characteristics of the subjects including age, gender, weight, and height, body mass index are presented in Table XII.

The boxplot of absolute error between Respinos and the reference devices for four vital signs is shown in Figure 24. Compared with the reference devices, Respinos yielded MAE of 2.07 ± 1.59 , 1.32 ± 1.07 , 0.21 ± 0.16 , and 1.12 ± 0.89 for RR, HR, temperature, and SpO2, respectively. These small error values indicate good performance of Respinos.

For spirometry mode of Respinos, it was successfully validated and certified by two independent institutions: Health Facility Security Center (HFSC), Jakarta (Certificate No. YK.01.03/XLVIII.2/PK/2022 023) and Global Quality Indonesia (GQI), Bandung (Certificate No. 00440/MD/GQI-Sert/02/22). In both certifications, Respinos was calibrated using Hans Rudolph volume calibration syringe 5530 [60]. Validation by HFSC on 0.5 and 3 L measurements yielded error percentages of 2.00% and 0.03%, respectively, whereas the validation by GQI on 0.5 and 3 L measurements yielded

TABLE X
SPIROMETER PARAMETER MEASUREMENTS.

No	FVC			FEV1			FEV1/FVC			PEFR		
	Respinos	Reference	Error (%)	Respinos	Reference	Error (%)	Respinos	Reference	Error (%)	Respinos	Reference	Error (%)
1	4.59	4.57	0.44	3.86	3.85	0.26	84.00	84.20	0.24	9.66	9.27	4.21
2	4.58	4.49	2.00	3.91	3.96	1.26	85.00	88.20	3.63	8.45	8.24	2.55
3	4.55	4.59	0.87	3.98	4.15	4.10	87.00	90.30	3.65	8.65	8.59	0.70
Average	4.57	4.55	0.51	3.92	3.99	1.76	85.33	87.57	2.55	8.92	8.70	2.53

TABLE XI
SPIROMETRY MEASUREMENT RESULTS USING RESPINOS.

Parameter	Unit	Pred	Test 1		Test 2		Test 3	
			Value	%Pred	Value	%Pred	Value	%Pred
FVC	L	2.52	2.58	102.26	2.56	101.67	2.57	101.90
FEV1	L	2.24	2.09	93.22	2.03	90.46	2.07	92.20
FEV1/FVC	%	88.99	81.00	91.02	79.00	88.78	80.00	89.90
PEFR	L/s	6.73	4.51	67.06	4.55	67.66	4.34	64.54

TABLE XII
CHARACTERISTICS OF THE SUBJECTS.

Characteristics	Statistics
No. subjects	97
No. measurements per subject	60
Age (year)	31.8 ± 5.5
No. male (%)	76 (78.4%)
No. female (%)	21 (21.6%)
Height (cm)	166.4 ± 5.9
Weight (kg)	65.3 ± 6.6
Body mass index (kg/m ²)	23.7 ± 3.0

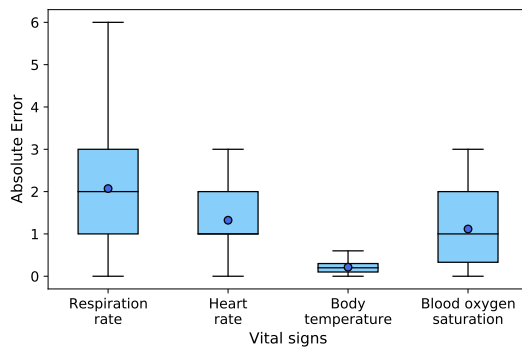


Fig. 24. Vital signs measurement error. The horizontal line and circle mark inside each boxplot denote the median and mean, respectively. The colored solid box represents interquartile range (IQR, 25th - 75th percentiles) with the whisker extending to 1.5 times the IQR.

error percentages of 1.20% and 0.37%, respectively. These results are below 3% which is the threshold for passing certification. The overall results demonstrate that Respinos has good performance and has potential to be used as remote patient monitoring device.

VII. CONCLUSION

In this study, a portable device, referred to as Respinos, to monitor multiparameter vital signs of COVID-19 patients, such as SpO₂, heart rate, respiratory rate, body temperature, and

lung capacity has been successfully designed, implemented and tested with a good accuracy. The lung capacity and parameters such as FVC, FEV1, FEV1/FVC and PEFR were measured using Respinos' spirometer mode. The experiment results in lab and clinical trial showed that average errors are low compared to reference device, indicating its good performance. Respinos is connected to a smartphone application via bluetooth and to the cloud via WiFi, which enables doctors to monitor remotely the progression of the patients' health. This reduces the risk of virus transmission which is very suitable for remote monitoring of COVID-19 patients either at home or clinic. It is portable, low cost and low power consumption, and can be used as a diagnostic or monitoring device that supports telehealth system during and post-pandemic.

REFERENCES

- [1] S. Bhaskar, S. Bradley, V. K. Chattu, A. Adishes, A. Nurtazina, S. Kyrk-bayeva, S. Sakhamuri, S. Yaya, T. Sunil, P. Thomas, *et al.*, "Telemedicine across the globe-position paper from the COVID-19 pandemic health system resilience PROGRAM (REPROGRAM) international consortium (part 1)," *Frontiers in Public Health*, p. 644, 2020.
- [2] WHO, "WHO coronavirus (COVID-19) dashboard," Accessed on: March 29, 2022. [Online]. Available: <https://covid19.who.int/>
- [3] X. Ding, D. Clifton, N. Ji, N. H. Lovell, P. Bonato, W. Chen, X. Yu, Z. Xue, T. Xiang, X. Long, *et al.*, "Wearable sensing and telehealth technology with potential applications in the coronavirus pandemic," *IEEE Reviews in Biomedical Engineering*, vol. 14, pp. 48–70, 2020.
- [4] Q. Ma, J. Liu, Q. Liu, L. Kang, R. Liu, W. Jing, Y. Wu, and M. Liu, "Global percentage of asymptomatic SARS-CoV-2 infections among the tested population and individuals with confirmed COVID-19 diagnosis: a systematic review and meta-analysis," *JAMA Network Open*, vol. 4, no. 12, pp. e2137257–e2137257, 2021.
- [5] Z. Wu and J. M. McGoogan, "Characteristics of and important lessons from the coronavirus disease 2019 (COVID-19) outbreak in China: summary of a report of 72 314 cases from the Chinese Center for Disease Control and Prevention," *JAMA*, vol. 323, no. 13, pp. 1239–1242, 2020.
- [6] D. R. Seshadri, E. V. Davies, E. R. Harlow, J. J. Hsu, S. C. Knighton, T. A. Walker, J. E. Voos, and C. K. Drummond, "Wearable sensors for COVID-19: a call to action to harness our digital infrastructure for remote patient monitoring and virtual assessments," *Frontiers in Digital Health*, p. 8, 2020.
- [7] M. Michelen, L. Manoharan, N. Elkheir, V. Cheng, A. Dagens, C. Hastie, M. O'Hara, J. Suett, D. Dahmash, P. Bugaeva, *et al.*, "Characterising long COVID: a living systematic review," *BMJ Global Health*, vol. 6, no. 9, p. e005427, 2021.
- [8] P. Venkatesan, "NICE guideline on long COVID," *The Lancet Respiratory Medicine*, vol. 9, no. 2, p. 129, 2021.
- [9] H. Crook, S. Raza, J. Nowell, M. Young, and P. Edison, "Long COVID—mechanisms, risk factors, and management," *BMJ*, vol. 374, 2021.
- [10] N. Ji, T. Xiang, P. Bonato, N. H. Lovell, S.-Y. Ooi, D. A. Clifton, M. Akay, X.-R. Ding, B. P. Yan, V. Mok, *et al.*, "Recommendation to use wearable-based mhealth in closed-loop management of acute cardiovascular disease patients during the COVID-19 pandemic," *IEEE Journal of Biomedical and Health Informatics*, vol. 25, no. 4, pp. 903–908, 2021.

- [11] B. L. Graham, I. Steenbruggen, M. R. Miller, I. Z. Barjaktarevic, B. G. Cooper, G. L. Hall, T. S. Hallstrand, D. A. Kaminsky, K. McCarthy, M. C. McCormack, *et al.*, "Standardization of spirometry 2019 update. an official american thoracic society and european respiratory society technical statement," *American Journal of Respiratory and Critical Care Medicine*, vol. 200, no. 8, pp. e70–e88, 2019.
- [12] D. P. Johns, J. A. Walters, and E. H. Walters, "Diagnosis and early detection of COPD using spirometry," *Journal of Thoracic Disease*, vol. 6, no. 11, p. 1557, 2014.
- [13] B. F. Nobakht M. Gh, R. Aliannejad, M. Rezaei-Tavirani, S. Taheri, and A. A. Oskouie, "The metabolomics of airway diseases, including COPD, asthma and cystic fibrosis," *Biomarkers*, vol. 20, no. 1, pp. 5–16, 2015.
- [14] J. Budd, B. S. Miller, E. M. Manning, V. Lampos, M. Zhuang, M. Edelstein, G. Rees, V. C. Emery, M. M. Stevens, N. Keegan, *et al.*, "Digital technologies in the public-health response to COVID-19," *Nature Medicine*, vol. 26, no. 8, pp. 1183–1192, 2020.
- [15] H. Lukas, C. Xu, Y. Yu, and W. Gao, "Emerging telemedicine tools for remote COVID-19 diagnosis, monitoring, and management," *ACS Nano*, vol. 14, no. 12, pp. 16180–16193, 2020.
- [16] A. Channa, N. Popescu, J. Skibinska, and R. Burget, "The rise of wearable devices during the COVID-19 pandemic: A systematic review," *Sensors*, vol. 21, no. 17, p. 5787, 2021.
- [17] K. Zhang and W. Ling, "Health monitoring of human multiple physiological parameters based on wireless remote medical system," *IEEE Access*, vol. 8, pp. 71146–71159, 2020.
- [18] A. Raposo, L. Marques, R. Correia, F. Melo, J. Valente, T. Pereira, L. B. Rosário, F. Froes, J. Sanches, and H. P. d. Silva, "e-CoVig: a novel mHealth system for remote monitoring of symptoms in COVID-19," *Sensors*, vol. 21, no. 10, p. 3397, 2021.
- [19] O. Taiwo and A. E. Ezugwu, "Smart healthcare support for remote patient monitoring during COVID-19 quarantine," *Informatics in Medicine Unlocked*, vol. 20, p. 100428, 2020.
- [20] W. Jiang, S. Majumder, S. Kumar, S. Subramaniam, X. Li, R. Khedri, T. Mondal, M. Abolghasemian, I. Satia, and M. J. Deen, "A wearable tele-health system towards monitoring COVID-19 and chronic diseases," *IEEE Reviews in Biomedical Engineering*, vol. 15, pp. 61–84, 2021.
- [21] N. Al Bassam, S. A. Hussain, A. Al Qaraghuli, J. Khan, E. Sumesh, and V. Lavanya, "IoT based wearable device to monitor the signs of quarantined remote patients of COVID-19," *Informatics in Medicine Unlocked*, vol. 24, p. 100588, 2021.
- [22] F. M. Iqbal, M. Joshi, G. Davies, S. Khan, H. Ashrafian, and A. Darzi, "Design of the pilot, proof of concept REMOTE-COVID trial: remote monitoring use in suspected cases of COVID-19 (SARS-CoV-2)," *Pilot and Feasibility Studies*, vol. 7, no. 1, pp. 1–7, 2021.
- [23] M. U. H. Al Rasyid, M. Sulistiyo, S. Sukaridhoto, *et al.*, "Design and development of portable spirometer," in *2018 IEEE International Conference on Consumer Electronics-Taiwan (ICCE-TW)*. IEEE, 2018, pp. 1–2.
- [24] S. Trivedy, M. Goyal, P. R. Mohapatra, and A. Mukherjee, "Design and development of smartphone-enabled spirometer with a disease classification system using convolutional neural network," *IEEE Transactions on Instrumentation and Measurement*, vol. 69, no. 9, pp. 7125–7135, 2020.
- [25] D. M. Carpenter, R. Jurdi, C. A. Roberts, M. Hernandez, R. Horne, and A. Chan, "A review of portable electronic spirometers: implications for asthma self-management," *Current allergy and asthma reports*, vol. 18, no. 10, pp. 1–10, 2018.
- [26] C. Ramos Hernández, M. Núñez Fernández, A. Pallares Sanmartín, C. Mouronte Roibas, L. Cerdeira Domínguez, M. I. Botana Rial, N. Blanco Cid, and A. Fernández Villar, "Validation of the portable air-smart spirometer," *PLoS one*, vol. 13, no. 2, p. e0192789, 2018.
- [27] P. Zhou, L. Yang, and Y.-X. Huang, "A smart phone based handheld wireless spirometer with functions and precision comparable to laboratory spirometers," *Sensors*, vol. 19, no. 11, p. 2487, 2019.
- [28] K. P. Exarchos, A. Gogali, A. Sioutkou, C. Chronis, S. Peristeri, and K. Kostikas, "Validation of the portable Bluetooth® Air Next spirometer in patients with different respiratory diseases," *Respiratory Research*, vol. 21, no. 1, pp. 1–7, 2020.
- [29] P. S. Shinde, R. R. Kulkarni, and G. V. Kulkarni, "Validation of portable Bluetooth enabled smart spirometer (Alveoair) for the measurement of various lung functions in healthy subjects," *National Journal of Physiology, Pharmacy and Pharmacology*, vol. 11, no. 10, pp. 1152–1152, 2021.
- [30] Medical International Research, "Spirobank Smart," Accessed 19 July 2022. [Online]. Available: <https://spirometry.com/en/products/spirobank-smart/>
- [31] NuvoAir, "Air Next spirometer," Accessed 27 July 2022. [Online]. Available: <https://www.nuvoair.com/for-providers>
- [32] Alveofit, "Manage your respiratory health with alveoair," Accessed 27 July 2022. [Online]. Available: <https://www.alveo.fit/alveoair/>
- [33] Medical International Research, "Spirobank Oxi," Accessed 19 July 2022. [Online]. Available: <https://spirometry.com/en/products/spirobank-oxi/>
- [34] Vyaire Medical, "AioCare Respiratory Disease Management System," Accessed 19 July 2022. [Online]. Available: <https://intl.vyaire.com/products/aiocare-respiratory-disease-management-system>
- [35] P. Sridevi, P. Kundu, T. Islam, C. Shahnaz, and S. A. Fattah, "A low-cost venturi tube spirometer for the diagnosis of COPD," in *TENCON 2018-2018 IEEE Region 10 Conference*. IEEE, 2018, pp. 0723–0726.
- [36] R. Sanga, A. Mittal, N. Samane, M. Sivaramakrishna, and G. P. Rao, "Design and development of quasi digital sensor based spirometer," in *Journal of Physics: Conference Series*, vol. 1921, no. 1. IOP Publishing, 2021, p. 012044.
- [37] Maxim Integrated, "DS18B20 - Programmable Resolution 1-Wire Digital Thermometer," Accessed on 29 April 2022. [Online]. Available: <https://datasheets.maximintegrated.com/en/ds/DS18B20.pdf>
- [38] Espressif Systems, "ESP32 Series Datasheet," Accessed on 29 April 2022. [Online]. Available: https://www.espressif.com/sites/default/files/documentation/esp32_datasheet_en.pdf
- [39] Texas Instruments, "AFE4400 - Integrated Analog Front-End for Heart Rate Monitors and Low-Cost Pulse Oximeters," Accessed on 29 April 2022. [Online]. Available: <https://www.ti.com/lit/ds/symlink/afe4400.pdf>
- [40] Microchip Technology, "Atmel 8-bit AVR Microcontroller with 2/4/8K Bytes In-System Programmable Flash," Accessed on 29 April 2022. [Online]. Available: <https://ww1.microchip.com/downloads/en/DeviceDoc/Atmel-2586-AVR-8-bit-Microcontroller-ATtiny25-ATtiny45-ATtiny85-Datasheet.pdf>
- [41] K. Gunawardena, K. Houston, and A. Smith, "Evaluation of the turbine pocket spirometer," *Thorax*, vol. 42, no. 9, pp. 689–693, 1987.
- [42] L. Malmberg, J. Hedman, and A. Sovijärvi, "Accuracy and repeatability of a pocket turbine spirometer: comparison with a rolling seal flow-volume spirometer," *Clinical Physiology*, vol. 13, no. 1, pp. 89–98, 1993.
- [43] K. Harri, R. S. Tapani, K. Senja, and K. Matti, "Hand-held turbine spirometer: Agreement with the conventional spirometer at baseline and after exercise," *Pediatric Allergy and Immunology*, vol. 16, no. 3, pp. 254–257, 2005.
- [44] O. Pedersen, M. Miller, T. Sigsgaard, M. Tidley, and R. Harding, "Portable peak flow meters: physical characteristics, influence of temperature, altitude, and humidity," *European Respiratory Journal*, vol. 7, no. 5, pp. 991–997, 1994.
- [45] S. Bagchi, S. Sengupta, and S. Mandal, "Development and characterization of a wireless mouse-based spirometer," *IEEE Sensors Journal*, vol. 17, no. 7, pp. 2065–2073, 2017.
- [46] Y. Sokol, R. Tomashevsky, and K. Kolisnyk, "Turbine spirometers metrological support," in *2016 International Conference on Electronics and Information Technology (EIT)*. IEEE, 2016, pp. 1–4.
- [47] Sensirion, "SFM3000-200 - versatile low pressure drop digital flow sensor," Accessed on: March 16, 2022. [Online]. Available: <https://sensirion.com/products/catalog/SFM3000-200/>
- [48] J. A. Pologe, "Pulse oximetry: technical aspects of machine design," *International Anesthesiology Clinics*, vol. 25, no. 3, pp. 137–153, 1987.
- [49] MQTT, "MQTT: The Standard for IoT Messaging," Accessed on 29 April 2022. [Online]. Available: <https://mqtt.org/>
- [50] JSON, "Introducing JSON," Accessed on 29 April 2022. [Online]. Available: <https://www.json.org/>
- [51] RESTful API, "What is REST," Accessed on 29 April 2022. [Online]. Available: <https://restfulapi.net/>
- [52] MongoDB, "Mongodb: The application data platform," Accessed 29 April 2022. [Online]. Available: <https://www.mongodb.com/>
- [53] Mosquitto, "Eclipse mosquitto: An open source mqtt broker," Accessed on 29 April 2022. [Online]. Available: <https://mosquitto.org/>
- [54] Fluke Biomedical, "ProSim SPOT Light SpO2 Pulse Oximeter Tester," Accessed on: March 31, 2022. [Online]. Available: <https://www.flukebiomedical.com/products/biomedical-test-equipment/patient-monitor-simulators/prosim-spot-light-spo2-pulse-oximeter-tester>
- [55] —, "Fluke 88V Deluxe Automotive Multimeter," Accessed 29 April 2022. [Online]. Available: <https://www.fluke.com/en-id/product/electrical-testing/digital-multimeters/fluke-88v>
- [56] Omron Healthcare, "Digital Thermometer MC-343F," Accessed 29 April 2022. [Online]. Available: <https://www.omronhealthcare-ap.com/id/product/260-mc-343f>

- [57] CONTEC, "CONTEC SP80B Spirometer," Accessed on: March 31, 2022. [Online]. Available: <https://contechhealth.com/products/contec-sp80b>
- [58] Microlife, "MT 200 Digital Thermometer," Accessed 27 July 2022. [Online]. Available: <https://www.microlife.com/support/fever/mt-200>
- [59] Mindray, "Patient Monitor Mindray Beneview T8," Accessed 27 July 2022. [Online]. Available: <https://www.mindray.com/id/product/beneview-t5-t6-t8-t9.html>
- [60] Hans Rudolph, "Volume Calibration Syringes," Accessed 27 July 2022. [Online]. Available: <https://www.rudolphkc.com/product-page/calibration-syringes>



Trio Adiono (Member, IEEE) received the B.Eng. degree in electrical engineering and the M.Eng. degree in microelectronics from Bandung Institute of Technology (ITB), Indonesia, in 1994 and 1996, respectively, and the Ph.D. degree in VLSI design from Tokyo Institute of Technology, Japan, in 2002. He is currently a Professor at the School of Electrical Engineering and Informatics and also serves as the Head for the IC Design Laboratory, Microelectronics Center, ITB. He holds a Japanese patent on a high quality video compression system. His research inter-

ests include VLSI design, signal and image processing, VLC, smart cards, and electronics solution design and integration.



Nur Ahmadi (Member, IEEE) received the B.Eng. degree in electrical engineering from Bandung Institute of Technology (ITB), Indonesia, in 2011 and M.Eng. degree in communication and integrated systems from Tokyo Institute of Technology, Japan, in 2013. He received his Ph.D. degree in Electrical and Electronic Engineering from Imperial College London, UK, in 2020. His Ph.D. research focused on signal processing and deep learning for intracortical brain-machine interfaces. He is now with the Center for Artificial Intelligence and School of Electrical

Engineering and Informatics, Institut Teknologi Bandung. His current research interests include biomedical signal processing, artificial intelligence, machine learning, digital and embedded systems.



Citrya Saraswati received a B.Eng. degree in electrical engineering from Bandung Institute of Technology (ITB), Indonesia in 2014. She currently works as a Hardware Designer at Xirka, Indonesia. She has broad experience and knowledge in digital circuit design using FPGA or embedded microcontroller, product development and prototyping including sketch design requirement, schematic design, PCB layout, embedded programming and VLSI design.



and RF design.

Yusuf P. Yudhanto received a B.Eng. degree in electrical engineering from Bandung Institute of Technology (ITB), Indonesia in 2009. He currently works as a Head of Hardware Designer at Xirka, Indonesia. He is experienced in analog RF HF/UHF and digital circuit design using FPGA or embedded microcontroller. He has broad knowledge in hardware prototyping to production, including sketch design requirement, schematic design, PCB layout, embedded programming and VLSI Design. His main works include VLSI design, embedded controller



Abdillah Aziz received a B.Eng. degree in electrical engineering from Bandung Institute of Technology (ITB), Indonesia in 2009. He worked as a Product and Test Engineer at Infineon Technologies, Indonesia from 2014 to 2016. In 2017, he joined Xirka, Indonesia as a Test Engineer and then Product Manager. He has experience in analog chip test scenario development and evaluation, chip package development, and medical device development.



Yudi Aditya earned a bachelor's degree in mathematics education from Indonesia University of Education (UPI) in 2012. He continued master's education at the Computational Science Study Program, Bandung Institute of Technology (ITB) in 2017. At the end of his master's education, he joined an Erasmus program in informatics engineering at the Universidad de Lleida, Spain. He currently works as a software engineer at Xirka, Indonesia.



Laksmi Wulandari received a Ph.D. degree in pulmonary medicine in 2014. She is a member of several professional associations including The Indonesian Association of Physicians (IDI) since 2000, Fellow of American College of Chest Physician (FCCP) since 2010, International Association for The Study of Lung Cancer (IASLC) since 2015, Fellow of The Indonesian Society of Community Medicine (FISCM) 2016, Fellow of Indonesian Society of Respiriology (FISR) since 2019. She is a senior lecturer in Pulmonology and Respiratory Medicine Department, Dr. Soetomo General Academic Hospital, Universitas Airlangga School of Medicine, Surabaya. She currently serves as the chairs of Thoracic Oncology Division.



Daniel Maranatha is a Consultant Pulmonary Physician for Asthma and COPD who was born in Surabaya, June 23, 1955. He completed his education in Pulmonology and Respiratory Medicine (Lung) Specialist at Airlangga University, Surabaya (1993)



Gemilang Khusnurrokhman obtained his MD in 2015 from Medical Faculty of Mataram University - RSUD Province of NTB. He was a Chief of Internship Medical Doctor for NTB Regional from November 2015-2016. He was also an assistant MD in Dept. Pulmonology and Respiratory Medicine from February 2017 - July 2017 at RSUD Province of NTB. Currently, he is a Chief Resident in his third level of Pulmonology and Respiratory Medicine in Airlangga University - Soetomo General Hospital since 2018. His research interests are interventional

pulmonology, thoracic oncology and pulmonary fibrosis.



Agustinus Rizki Wirawan Riadi obtained his MD in 2011 from Medical Faculty of Wijaya Kusuma University. He worked in the Navy Hospital from 2012 to 2018. He is taking pulmonology education from 2018 to present. Currently, he is the chief in his third level of pulmonology and respiratory medicine resident at the University of Airlangga. His research interests are thoracic oncology, interventional pulmonology and pulmonary infection.



Reza Widiyanto Sudjud received his degree in anesthesiology in 2010, cardiothoracic anesthesia in 2013, and intensive care medicine in 2015, from the University of Padjajaran, Bandung, Indonesia. He obtained his doctorate degree in 2018. He is now the head of Cardiothoracic Anesthesia Fellowship Program in RSUP Dr. Hasan Sadikin, Study Coordinator of Intensive Care Medicine program and staff in Anesthesiology and Intensive Care program in University of Padjajaran. His research interests include cardiac anesthesia and intensive care medicine.



**KOMITE ETIK PENELITIAN KESEHATAN
RSUD Dr. SOETOMO SURABAYA**

**KETERANGAN KELAIKAN ETIK
(" ETHICAL CLEARANCE ")**

0239/KEPK/VIII/2021

**KOMITE ETIK RSUD Dr. SOETOMO SURABAYA TELAH MEMPELAJARI
SECARA SEKSAMA RANCANGAN PENELITIAN YANG DIUSULKAN, MAKA
DENGAN INI MENYATAKAN BAHWA PENELITIAN DENGAN JUDUL :**

" PERANGKAT DIAGNOSIS RESPIRASI PORTABLE COVID-19 "

PENELITI UTAMA : Dr. Laksmi Wulandari, dr., Sp.P (K)

PENELITI LAIN : 1. Dr. Daniel Maranatha, dr., Sp.P (K)

2. Prof. Trio Adiono, S.T., M.T., Ph.D

3. Dr. Reza Widiyanto Sudjud, dr., Sp.An., KAKV., KIC., M.Kes

4. Gemilang Khusnurrokhman, dr

5. Agustinus rizki Wirawan Riadi, dr

6. Dr. Arto Yuwono Soeroto, dr., Sp.PD-KP., FINASIM., FCCP

7. Hana Nur Ramila, dr., Sp.An

8. M. Budi Kurniawan, dr., Sp.An., FCTA

UNIT / LEMBAGA / TEMPAT PENELITIAN : RSUD Dr. Soetomo

RSUP Dr. Hasan Sadikin

DINYATAKAN LAIK ETIK

Berlaku dari : 20/08/2021 s.d 20/08/2022

Surabaya, 20 Agustus 2021

KETUA



(Prof. Dr. Hendy Hendarto, dr., SpOG (K))

NIP. 19610817 201601 6 101

***) Sertifikat ini dinyatakan sah apabila telah mendapatkan stempel asli dari Komite Etik Penelitian Kesehatan**